

Supporting Information

for

Targeted Attachment of Functional Groups at Ge₉ Clusters via Silylation Reactions

Kerstin Mayer, Lorenz J. Schiegerl, Tim Kratky, Sebastian Günther, and Thomas F. Fässler

Contents

- 1 Experimental Details
- 2 NMR Spectra
- 3 ESI-MS Spectra
- 4 IR and Raman Spectra
- 5 XPS Investigations
- 6 Crystallographic Details
- 7 Literature

1. Experimental Details

General. All reactions and manipulations were performed under a purified argon atmosphere using standard Schlenk and glove box techniques. The Zintl compound of nominal composition K₄Ge₉ was synthesized by heating (2 K/min) of a stoichiometric mixture of the elements K (Merck, ≥98%) and Ge (99.999% Chempur) at 650 °C in a stainless steel autoclave for 46 h and slow cooling (1 K/min) to room temperature. Acetonitril (acn) and toluene were dried over molecular sieve (3 Å, 4 Å), thf over a special drying material in a solvent purificator (MBraun MB-SPS). The bis-silylated Ge₉ cluster K₂[Ge₉{Si(SiMe₃)₃}₂] was prepared according to literature.¹ ClSiPh₂CH=CH₂ and ClSiPh₂(CH₃)₃CH=CH₂ were synthesized after a modified literature method.² All chemicals were received commercially and used without further purification.

CISiPh₂CH=CH₂. To a diethyl ether solution of 12 mL (94.4 mmol, 1.05 equiv.) Cl₃SiCH=CH₂, 120 mL (180 mmol, 2 equiv.) of a 1.5 M Grignard-Solution of PhMgBr in thf is added over a period of 2 h at 0 °C. The reaction is completed by refluxing for 7 h. After filtration and removing of the solvent the residue is distilled under reduced pressure. 14.6 g (59.6 mmol, 66%) of a clear liquid are obtained at 103 °C (8 · 10⁻² mbar).

¹H-NMR (400 MHz, C₆D₆, 297 K): δ = 7.59-7.67 (m, 4H, H_{Ar}), 7.05-7.20 (m, 6H, H_{Ar}), 6.28-6.44 (m, 1H, CH=CH₂), 5.86-6.03 (m, 2H, CH=CH₂); **¹³C NMR** (101 MHz, C₆D₆, 297 K): δ = 137.9 (s, CH=CH₂), 135.2 (s, C_{Ar}), 133.2 (s, C_{Ar}), 133.1 (s, C_{Ar}), 130.9 (s, C_{Ar}), 128.4 (s, CH=CH₂); **²⁹Si NMR** (79 MHz, C₆D₆, 297 K): δ = -1.22 (s).

CISiPh₂(CH₃)₃CH=CH₂. To a diethyl ether solution of 12 mL (115 mmol, 2.67 equiv.) Cl₂SiPh₂, 18 mL (43 mmol, 1 equiv.) of a 2 M Grignard-Solution of Pent-4-enylmagnesiumbromide in thf is added drop-wise at 0 °C. The reaction is completed by refluxing for 7 h. After filtration and removing of the solvent the residue is distilled under reduced pressure. 7.34 g (25.6 mmol, 50%) of a clear liquid are obtained in the temperature range of 108 - 129 °C (2 · 10⁻² mbar).

¹H-NMR (400 MHz, C₆D₆, 297 K): δ = 7.57-7.76 (m, 4H, H_{Ar}), 7.03-7.31 (m, 6H, H_{Ar}), 5.63 (ddt, 1H, J = 17.2 Hz, 10.5 Hz, 6.8 Hz, CH=CH₂), 4.90-5.04 (m, 2H, CH=CH₂), 1.89-2.05 (m, 2H, CH₂), 1.55-1.68 (m, 2H, CH₂), 1.18-1.33 (m, 2H, CH₂); **¹³C NMR** (101 MHz, C₆D₆, 297 K): δ = 138.3 (s, CH=CH₂), 135.0 (s, C_{Ar}), 134.7 (s, C_{Ar}), 134.4 (s, C_{Ar}), 134.2 (s, C_{Ar}), 130.7 (s, C_{Ar}), 128.5 (s, C_{Ar}), 115.4 (s, CH=CH₂), 37.1 (s, CH₂), 22.8 (s, CH₂), 16.3 (s, CH₂); **²⁹Si NMR** (79 MHz, C₆D₆, 297 K): δ = 10.9 (s).

K[Ge₉{Si(SiMe₃)₃]₂(SiPh₂CH=CH₂)] (1). 120 mg (96 μmol; 1 equiv.) of K₂[Ge₉{Si(SiMe₃)₃]₂] and 23 mg (96 μmol, 1 equiv.) CISiPh₂CH=CH₂ are dissolved in 3 mL thf. The red solution is stirred overnight. The solvent is removed *in vacuo* and redissolved in 3 mL toluene. After filtration compound **1** is crystalized at -32 °C as **1·(Tol)**_{1.23}. EDX measurements confirms the presence of the elements Ge, Si and K in the single crystals. ESI-MS measurements of the raw product (60% yield) in acn reveals the formation of the anion [Ge₉{Si(SiMe₃)₃]₂(SiPh₂CH=CH₂)⁻ as single species. NMR spectra (¹H, ¹³C, ²⁹Si) of the raw product confirm a quantitative reaction. **¹H-NMR** (400 MHz, thf-d₈, 297 K): δ = 7.61-7.67 (m, 4H, H_{Ar}), 7.10-7.15 (m, 6H, H_{Ar}), 6.48 (dd, J = 14.2, 26.0 Hz, 1H, CH=CH₂), 5.85 (dd, J = 3.9, 14.0 Hz, 1H, CH=CH₂), 5.69 (dd, J = 4.0, 19.8 Hz, 1H, CH=CH₂), 0.27 (s, 54H, Si(CH₃)₃); **¹³C NMR** (101 MHz,

thf-d₈, 297 K): δ = 142.0 (s, CH=CH₂), 141.2 (s, C_{Ar}), 137.2 (s, C_{Ar}), 133.1 (s, CH=CH₂), 128.7 (s, C_{Ar}), 127.7 (s, C_{Ar}), 3.4 (s, Si(CH₃)₃); ²⁹Si NMR (79 MHz, thf-d₈, 297 K): δ = 4.9 (s, SiPh₂CH=CH₂), -9.5 (s, Si(SiMe₃)₃), -106.8 (s, Si(SiMe₃)₃). IR (ATR): $\tilde{\nu}$ (cm⁻¹) = 3067 (w, Ar-H), 3048 (w, Ar-H), 2942 (m, -CH₃), 2883 (m, -CH₂-), 1625 (w, C=C, Ar), 1588 (m, C=C, Ar), 1427 (m, C-C-H), 1397 (m, C-C-H), 1238 (m, Si-C), 1048 (b, Si-O), 822 (s, C=C-H), 683 (s, Ar), 620 (m, Si-Si), 542 (m, Si-Si), 483 (m, Si-Si). Raman: $\tilde{\nu}$ (cm⁻¹) = 112 (m, Ge₉), 158 (s, Ge₉), 188 (w, Ge₉), 242 (m, Ge₉), 309 (w, Si-Si, Si-C), 627 (m, Si-C), 686 (m, Si-C), 742 (w, Si-Si), 997 (m, Ar). ESI-MS (negative mode, 4000 V, 300 °C): m/z = 1359 [Ge₉{Si(SiMe₃)₃}₂(SiPh₂CH=CH₂)]⁻.

K[Ge₉{Si(SiMe₃)₃}₂{SiPh₂(CH₃)₃CH=CH₂}] (2). 120 mg (96 μmol; 1 equiv.) of K₂[Ge₉{Si(SiMe₃)₃}₂] and 28 mg (96 μmol, 1 equiv.) ClSiPh₂(CH₃)₃CH=CH₂ are dissolved in 3 mL thf. The red solution is stirred overnight. The solvent is removed *in vacuo* and redissolved in 3 mL toluene. After filtration compound **2** is crystalized at -32 °C as **2**·(thf). EDX measurements confirm the presence of the elements Ge, Si and K in the single crystals. ESI-MS measurements of the raw product (65% yield) in acn reveal the formation of the anion [Ge₉{Si(SiMe₃)₃}₂(SiPh₂(CH₃)CH=CH₂)]⁻ as single species. NMR (¹H, ¹³C, ²⁹Si) spectra of the raw product confirm a quantitative reaction. ¹H-NMR (400 MHz, thf-d₈, 297 K): δ = 7.64-7.70 (m, 4H, H_{Ar}), 7.09-7.14 (m, 6H, H_{Ar}), 5.70-5.82 (m, 1H, CH=CH₂), 4.90 (d, J = 18.4 Hz, 1H, CH=CH₂), 4.82 (d, J = 10.5 Hz, 1H, CH=CH₂), 2.02 (q, J = 6.9 Hz, 2H, CH₂), 1.55-1.65 (m, 2H, CH₂), 1.15-1.22 (m, 2H, CH₂), 0.27 (s, 54H, Si(CH₃)₃); ¹³C NMR (101 MHz, thf-d₈, 297 K): δ = 142.2 (s, CH=CH₂), 140.4 (s, C_{Ar}), 136.9 (s, C_{Ar}), 129.8 (s, C_{Ar}), 129.1 (s, C_{Ar}), 128.6 (s, C_{Ar}), 127.7 (s, C_{Ar}), 114.6 (s, CH=CH₂), 38.8 (s, CH₂), 26.3 (s, CH₂), 20.9 (s, CH₂), 3.4 (s, Si(CH₃)₃); ²⁹Si NMR (79 MHz, thf-d₈, 297 K): δ = 13.5 (s, SiPh₂(CH₃)₃CH=CH₂), -9.5 (s, Si(SiMe₃)₃), -107.0 (s, Si(SiMe₃)₃). IR (ATR): $\tilde{\nu}$ (cm⁻¹) = 3067 (w, Ar-H), 3046 (w, Ar-H), 2942 (m, -CH₃), 2883 (m, -CH₂-), 1588 (m, C=C, Ar), 1425 (m, C-C-H), 1395 (m, C-C-H), 1240 (m, Si-C), 1056 (b, Si-O), 824 (s, C=C-H), 681 (s, Ar), 620 (m, Si-Si), 559 (m, Si-Si), 491 (m, Si-Si). Raman: $\tilde{\nu}$ (cm⁻¹) = 114 (m, Ge₉), 160 (s, Ge₉), 186 (w, Ge₉), 241 (m, Ge₉), 311 (w, Si-Si, Si-C), 627 (m, Si-C), 688 (m, Si-C), 746 (w, Si-Si), 998 (m, Ar). ESI-MS (negative mode, 4000 V, 300 °C): m/z = 1400 [Ge₉{Si(SiMe₃)₃}₂{SiPh₂(CH₃)₃CH=CH₂}]⁻.

K[Ge₉(SiPh₂CH=CH₂)₃] (3). 74 mg (300 μmol, 3 equiv.) ClSiPh₂CH=CH₂ are dissolved in acn (3 mL), and 81 mg (100 μmol, 1 equiv.) K₄Ge₉ are added. The reaction mixture

turns red instantly, is stirred overnight and filtered. ESI-MS investigations of the acn solution reveal the formation of the tris-silylated anion. NMR (^1H , ^{13}C , ^{29}Si) investigations the formation of pure compounds by showing only one set of silyl signals. **^1H NMR** (400 MHz, thf- d_8 , 297 K) δ = 7.53 (m, 4H, CH_{Ar}), 7.31 (m, 6H, CH_{Ar}), 6.44 (dd, J = 20.4, 14.8 Hz, 1H, $\text{CH}=\text{CH}_2$), 6.14 (dd, J = 14.8, 3.8 Hz, 1H, $\text{CH}=\text{CH}_2$), 5.78 (dd, J = 20.3, 3.8 Hz, 1H, $\text{CH}=\text{CH}_2$); **^{13}C NMR** (126 MHz, thf- d_8) δ = 137.1 (C_{Vinyl}), 136.9 (C_{Vinyl}), 136.6 (C_{Ar}), 135.7 (C_{Ar}), 130.8 (C_{Ar}), 128.7 (C_{Ar}); **^{29}Si NMR** (99 MHz, thf- d_8) δ = -20.8 ($\text{SiPh}_2\text{CH}=\text{CH}_2$); **ESI-MS** (negative mode, 4500 V, 300 °C): m/z = 1282 [$\text{Ge}_9(\text{SiPh}_2\text{CH}=\text{CH}_2)_3$] $^-$.

$\text{K}[\text{Ge}_9\{\text{SiPh}_2(\text{CH}_3)_3\text{CH}=\text{CH}_2\}_3]$ (4). 80 mg (300 μmol , 3 equiv.) $\text{ClSiPh}_2(\text{CH}_3)_3\text{CH}=\text{CH}_2$ are dissolved in acn (3 mL), and 81 mg (100 μmol , 1 equiv.) K_4Ge_9 are added. The reaction mixture turns red instantly, is stirred overnight and filtered. ESI-MS investigations of the acn solution reveal the formation of the tris-silylated anion. NMR (^1H , ^{13}C , ^{29}Si) investigations confirm the formation of pure compounds by showing only one set of silyl signals.

^1H NMR (400 MHz, thf- d_8 , 297K) δ = 7.53 (m, 4H, CH_{Ar}), 7.28 (m, 6H, CH_{Ar}), 5.64 (m, 1H, $\text{CH}=\text{CH}_2$), 4.85 (m, 2H $\text{CH}=\text{CH}_2$), 1.96 (q, J = 7.1 Hz, 2H, CH_2), 1.43 (dq, J = 11.8, 7.4 Hz, 2H, CH_2), 1.09 (m, 2H, CH_2); **^{13}C NMR** (101 MHz, thf- d_8) δ = 139.4 (C_{Vinyl}), 137.7 (C_{Vinyl}), 135.3 (C_{Ar}), 130.6 (C_{Ar}), 128.64 (C_{Ar}), 115.2 (C_{Ar}), 38.4 (CH_2), 23.7 (CH_2), 16.2 (CH_2); **^{29}Si NMR** (79 MHz, thf- d_8) δ = -12.2 ($\text{SiPh}_2(\text{CH}_3)_3\text{CH}=\text{CH}_2$); **ESI-MS** (negative mode, 5000 V, 300 °C): m/z = 1408 [$\text{Ge}_9\{\text{SiPh}_2(\text{CH}_3)_3\text{CH}=\text{CH}_2\}_3$] $^-$.

$\text{K}[\text{Ge}_9(\text{Si}(\text{SiMe}_3)_3)_2(\text{SiMe}_2\text{CH}=\text{CH}_2)]$. 12 mg $\text{ClSiPh}_2(\text{CH}_3)_3\text{CH}=\text{CH}_2$ (96 μmol , 1 equiv.) are dissolved in acn (3 mL), and 120 mg $\text{K}_2[\text{Ge}_9\{\text{Si}(\text{SiMe}_3)_3\}_2]$ (96 μmol , 1 equiv.) are added. The red solution is stirred overnight and filtered. ESI-MS measurements of the solution reveal the formation of the anion [$\text{Ge}_9(\text{SiPh}_3)_2(\text{SiMe}_2\text{CH}=\text{CH}_2)$] $^-$ as single species.

^1H -NMR (400 MHz, acn- d_3 , 297 K): δ = 6.37–6.07 (m, 1H, $\text{CH}=\text{CH}_2$), 5.83–5.60 (m, 2H, $\text{CH}=\text{CH}_2$), 0.39–0.01 (m, 60H, $\text{Si}(\text{CH}_3)_2(\text{CH}=\text{CH}_2)$, $\text{Si}(\text{CH}_3)_3$). **^{29}Si NMR** (79 MHz, acn- d_3 , 297 K): δ = -9.3 (s, $\text{Si}(\text{SiMe}_3)_3$), -106.9 (s, $\text{Si}(\text{SiMe}_3)_3$); **ESI-MS** (negative mode, 5000 V, 300 °C): m/z = 1235 [$\text{Ge}_9(\text{Si}(\text{SiMe}_3)_3)_2(\text{SiMe}_2\text{CH}=\text{CH}_2)$] $^-$.

K[Ge₉(SiPh₃)₂(SiPh₂CH=CH₂)]. 250 mg (306 μmol, 1 equiv.) K₄Ge₉ and 180 mg (612 μmol, 2 equiv.) ClSiPh₃ are dissolved in 5 mL acn. The dark brown solution is stirred for 2 days, filtered, and the solvent is removed *in vacuo*. After extraction with toluene 110 mg (93 μmol; 1 equiv) of a brownish solid is isolated and identified *via* NMR spectroscopy as K₂[Ge₉(SiPh₃)₂]. To this compound 23 mg (96 μmol, 1.03 equiv.) ClSiPh₂CH=CH₂ dissolved in 3 mL acn are added. The red-brown solution is stirred overnight, filtered and the solvent removed *in vacuo*. ESI-MS measurements of the solid reveal the formation of the anion [Ge₉(SiPh₃)₂(SiPh₂CH=CH₂)]⁻ as well as the trisilylated clusters [Ge₉(SiPh₃)₂]⁻ and [Ge₉(SiPh₃)(SiPh₂CH=CH₂)₂]⁻.

ESI-MS (negative mode, 4000 V, 300 °C): *m/z* = 1383 [Ge₉(SiPh₃)₂(SiPh₂CH=CH₂)]⁻.

Single-Crystal Structure Determination. Single crystals were fixed on a glass fiber with perfluorinated ether and positioned in a 150 K cold N₂ stream. For single crystal X-ray diffraction data collection, a STOE StadiVari diffractometer (Mo-K_α radiation) was used. The structures were solved by Direct Methods and refined by full-matrix least-squares calculations against *F*² using SHELX-2014.³ Non-hydrogen atoms were treated with anisotropic displacement parameters. For compound **1** the total amount of solvent molecules was determined by using the squeeze function.⁴

Energy Dispersive X-ray (EDX) analysis. Single crystals of compounds **1** and **2** were analyzed with a scanning electron microscope equipped with an energy dispersive X-ray analyzer (Hitachi TM-1000 Tabletop microscope).

NMR Spectroscopy. ¹H, ¹³C and ²⁹Si NMR spectra were recorded on a Bruker AVIII 400 FT system or on a Bruker AVIII 500c (*Bruker Corp.*) at 300 K. The chemical shifts are given in δ values (ppm), the coupling constants *J* in Hz. The signals of ¹H and ¹³C spectra were calibrated on the rest proton signal of the used deuterated solvents thf-*d*₈ and acn-*d*₃. Signal multiplicities are abbreviated as follows: s - singlet, d - doublet, t - triplet, q - quartet and m - multiplet. The spectra were evaluated with MestReNova⁵.

Electron Spray Mass Spectrometry (ESI-MS). The preparation of the samples for ESI-MS measurements was performed in a glove box. The solutions were diluted to a concentration of approx. 2.0·10⁻⁴ mmol/mL. The measurements were performed on a HCT instrument (*Bruker Corp.*). Analysis of the data was evaluated using the program Bruker Compass Data Analysis 4.0 SP 5 (*Bruker Corp.*). The dry gas temperature was

adjusted at 125 °C and the injection speed at 240 µl/h. Visualization of the spectra was done with the programs OriginPro 2015G (*Origin Lab Corp.*) and Excel 2015 (*Microsoft Corp.*).

Infrared (IR) spectroscopy. FT-IR spectra were recorded on a Bruker Alpha FT-IR spectrometer with an ATR geometry, using a diamond ATR unit under argon atmosphere. In order to assign the vibrational bands the following abbreviations were used: s – strong, m – medium, w – weak and b – broad.

Raman spectroscopy. Raman spectra were recorded on a Renishaw inVia Raman Microscope RE04 equipped with four different lasers (229, 488, 633, and 785 nm; max. 500 mW) and a CCD detector. All samples were measured in quartz capillaries. In order to assign the vibrational bands the following abbreviations were used: s – strong, m – medium, w – weak and b – broad.

X-ray photoelectron spectroscopy (XPS). X-ray photoelectron spectra were recorded on a *Leybold-Heraeus* LHS 10 spectrometer using a non-monochromatized Al- K_{α} source (1486.7 eV). K_4Ge_9 was pressed into a cavity and measured as a pellet. All other powder samples were dissolved in acetonitrile or toluene and coated on a sample holder by drop casting. The analyzer was operated at a constant pass energy of 100 eV leading to an energy resolution with a full width at half-maximum (fwhm) of ~1.2 eV. The energy scale of the spectra was not corrected for sample charging due to the absence of a unique reference signal. The oxidation states of germanium were determined by the Auger parameter ($a' = E_{kin}(L_3M_{45}M_{45}) + E_b(3d) = 1174.5$ eV or $a' = E_{kin}(L_3M_{45}M_{45}) + E_b(2p_{3/2}) = 2362.4$ eV for Ge(0)).⁶ All spectra were recorded in an ultra-high vacuum chamber at a pressure below 5×10^{-8} mbar. Core level spectra were deconvoluted by using Voigt functions and linear background subtraction.

2. NMR Spectra

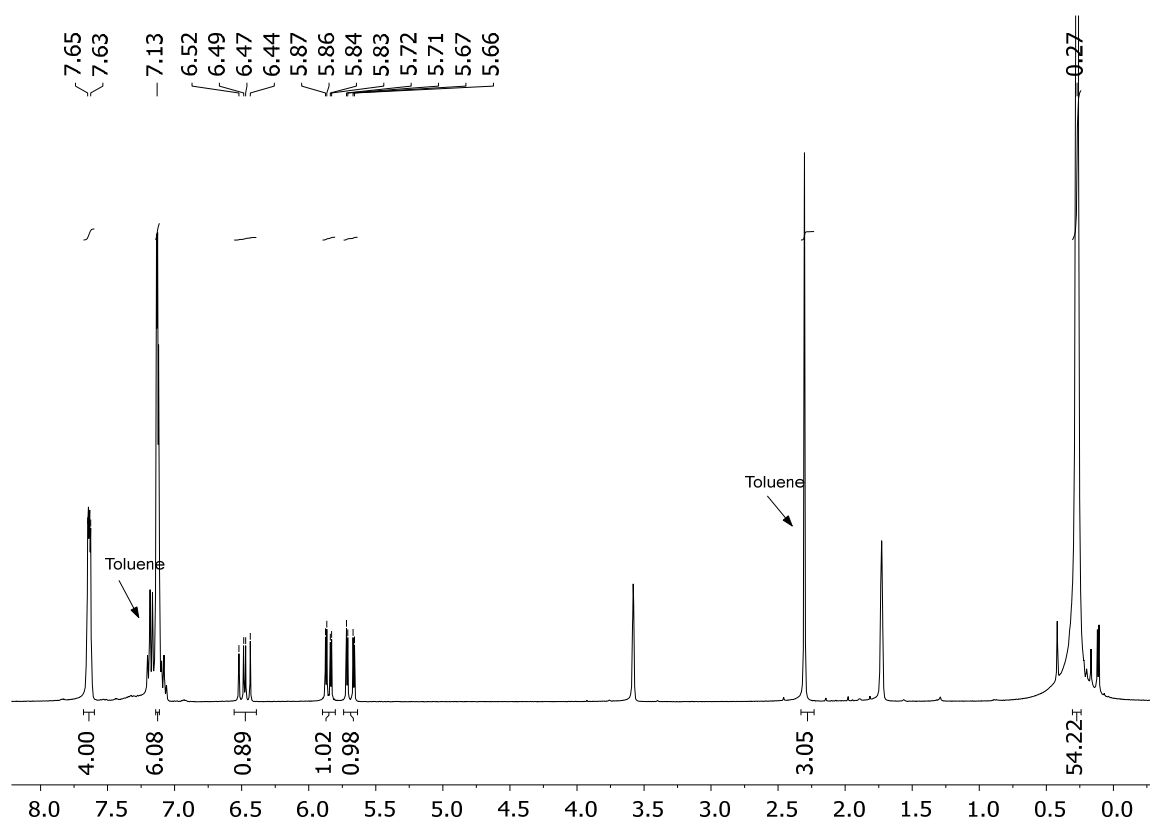


Figure S1: ^1H NMR spectrum of $\text{K}[\text{Ge}_9\{\text{Si}(\text{SiMe}_3)_3\}_2(\text{SiPh}_2\text{CH}=\text{CH}_2)]$ (**1**) in thf-d_8 .

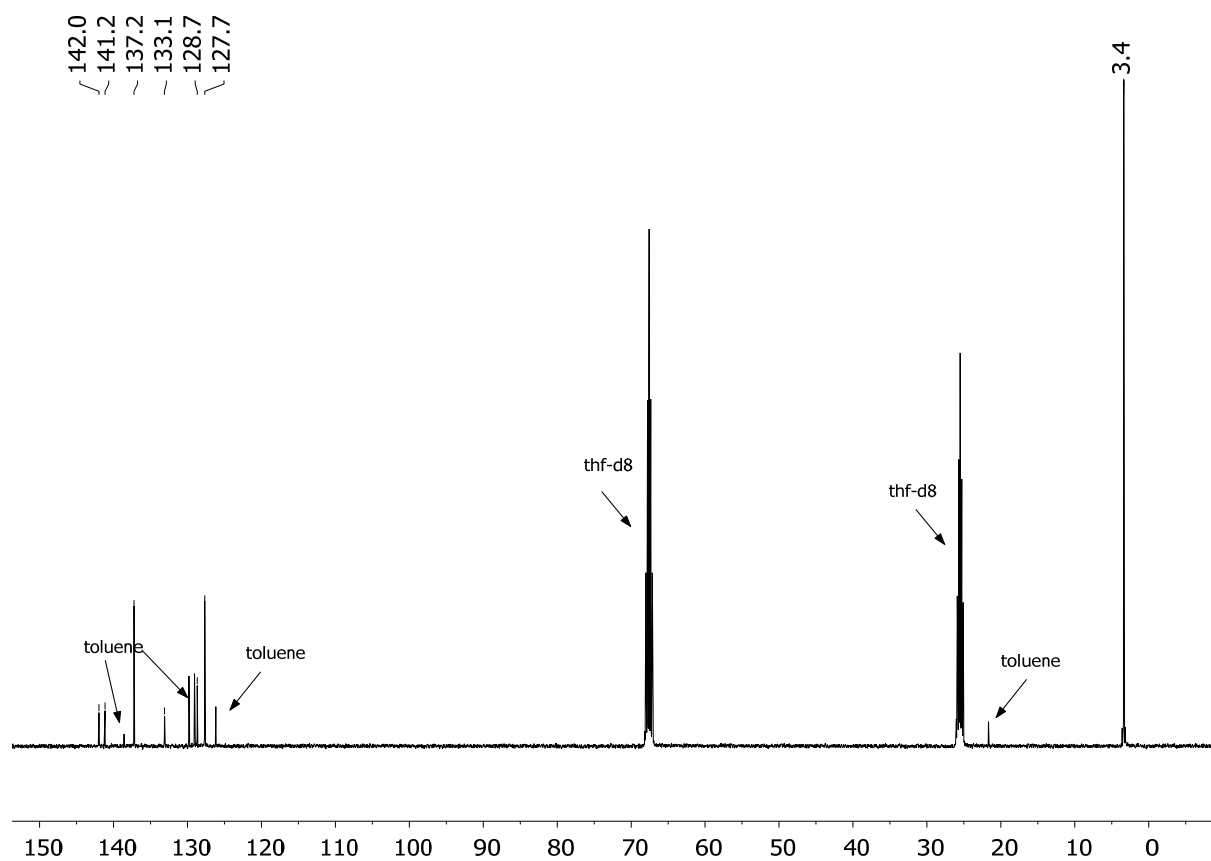


Figure S2: ^{13}C NMR spectrum of $\text{K}[\text{Ge}_9\{\text{Si}(\text{SiMe}_3)_3\}_2(\text{SiPh}_2\text{CH}=\text{CH}_2)]$ (**1**) in thf-d_8 .

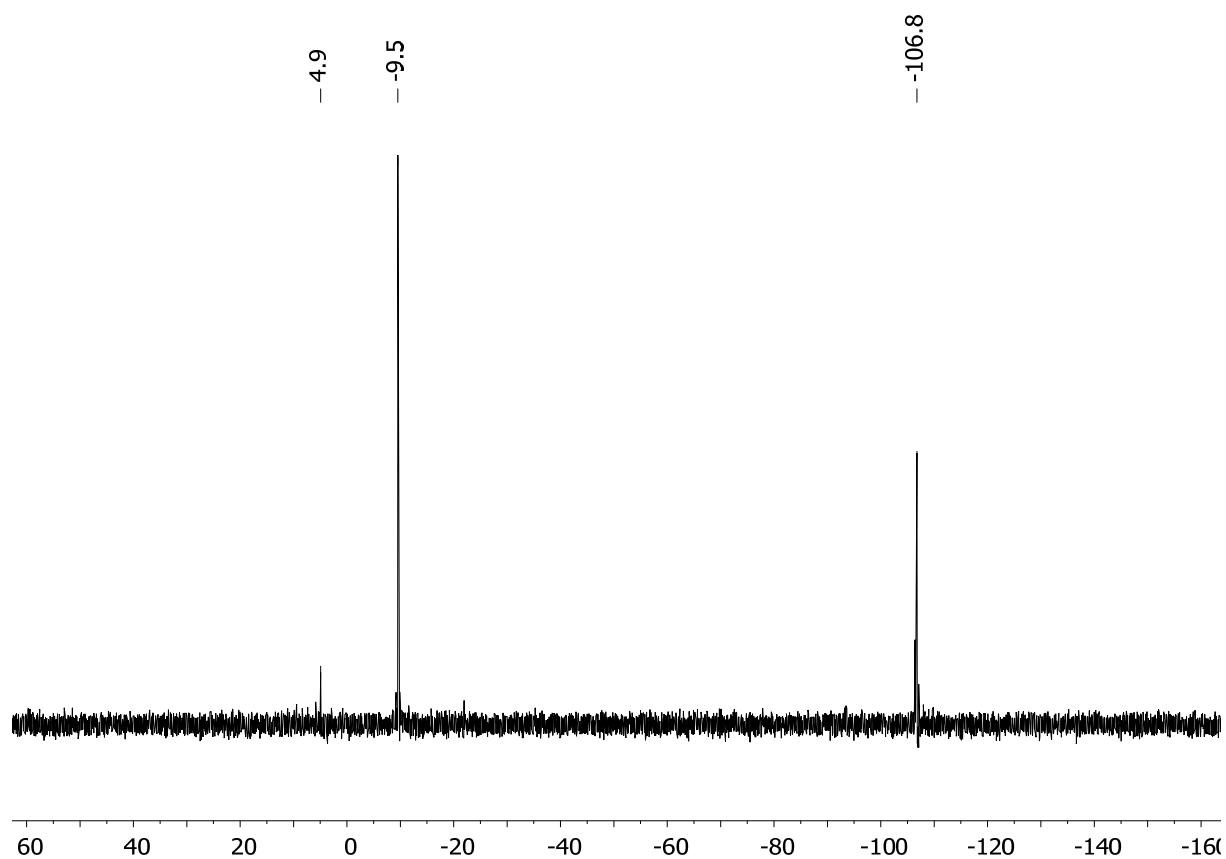


Figure S3: ^{29}Si NMR spectrum of $\text{K}[\text{Ge}_9\{\text{Si}(\text{SiMe}_3)_3\}_2(\text{SiPh}_2\text{CH}=\text{CH}_2)]$ (**1**) in thf-d_8 .

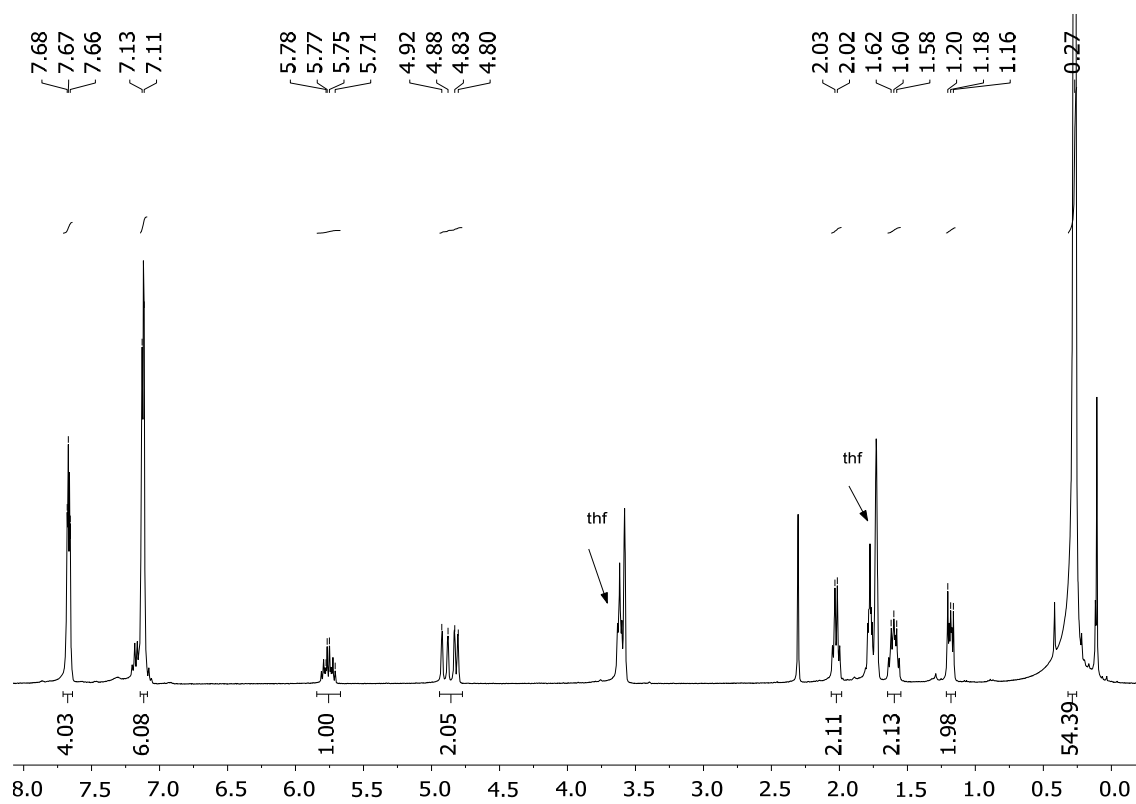


Figure S4: ^1H NMR spectrum of $\text{K}[\text{Ge}_9\{\text{Si}(\text{SiMe}_3)_3\}_2(\text{SiPh}_2(\text{CH}_2)_3\text{CH}=\text{CH}_2)]$ (**2**) in thf-d_8 .

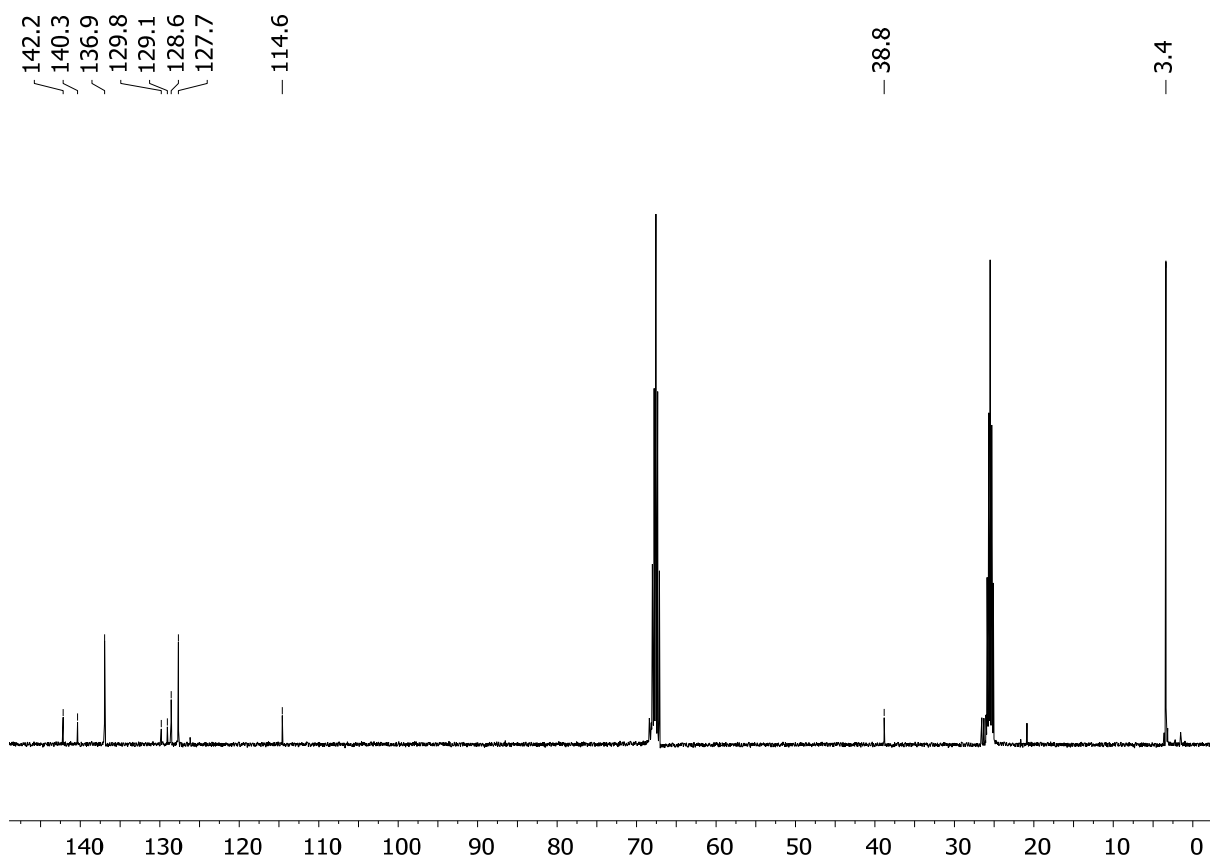


Figure S5: ¹³C NMR spectrum of $\text{K}[\text{Ge}_9\{\text{Si}(\text{SiMe}_3)_3\}_2(\text{SiPh}_2(\text{CH}_2)_3\text{CH}=\text{CH}_2)]$ (**2**) in thf-d_8 .

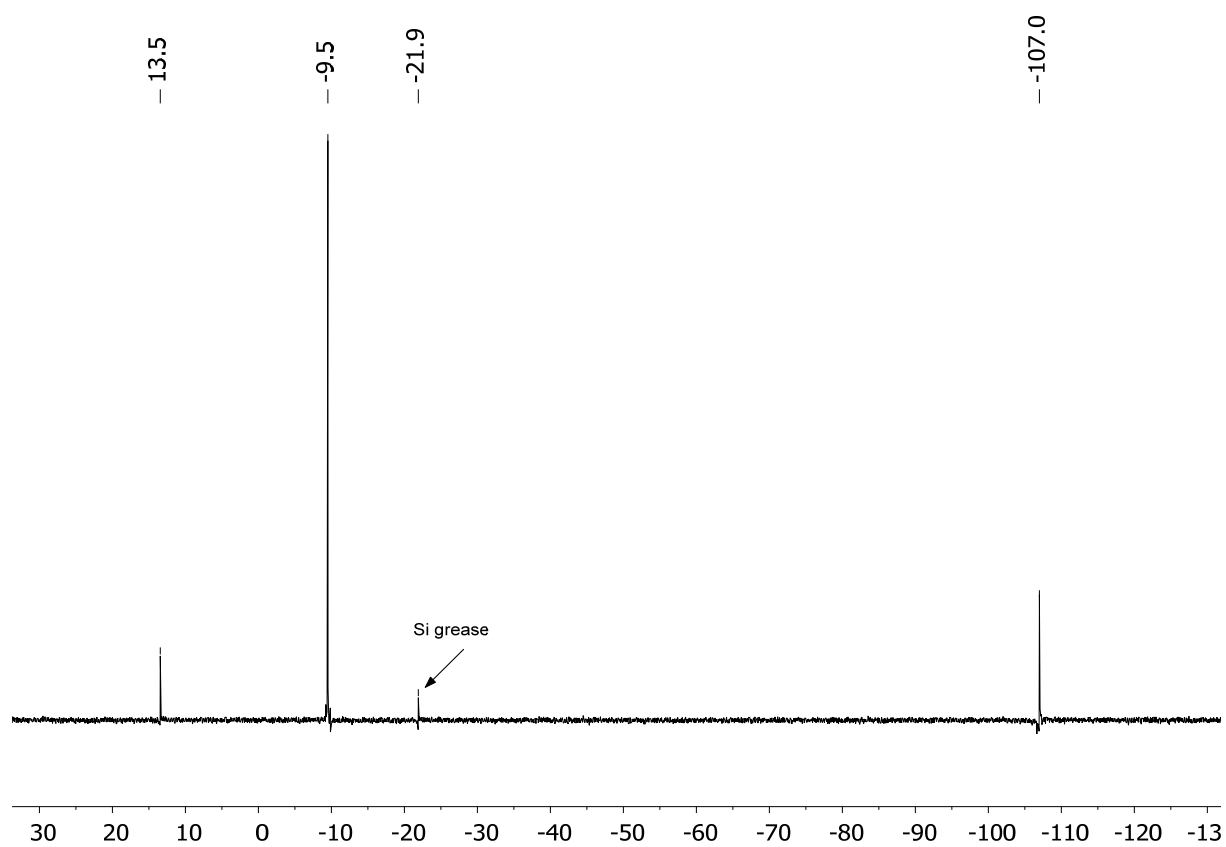


Figure S6: ²⁹Si NMR spectrum of $\text{K}[\text{Ge}_9\{\text{Si}(\text{SiMe}_3)_3\}_2(\text{SiPh}_2(\text{CH}_2)_3\text{CH}=\text{CH}_2)]$ (**2**) in thf-d_8 .

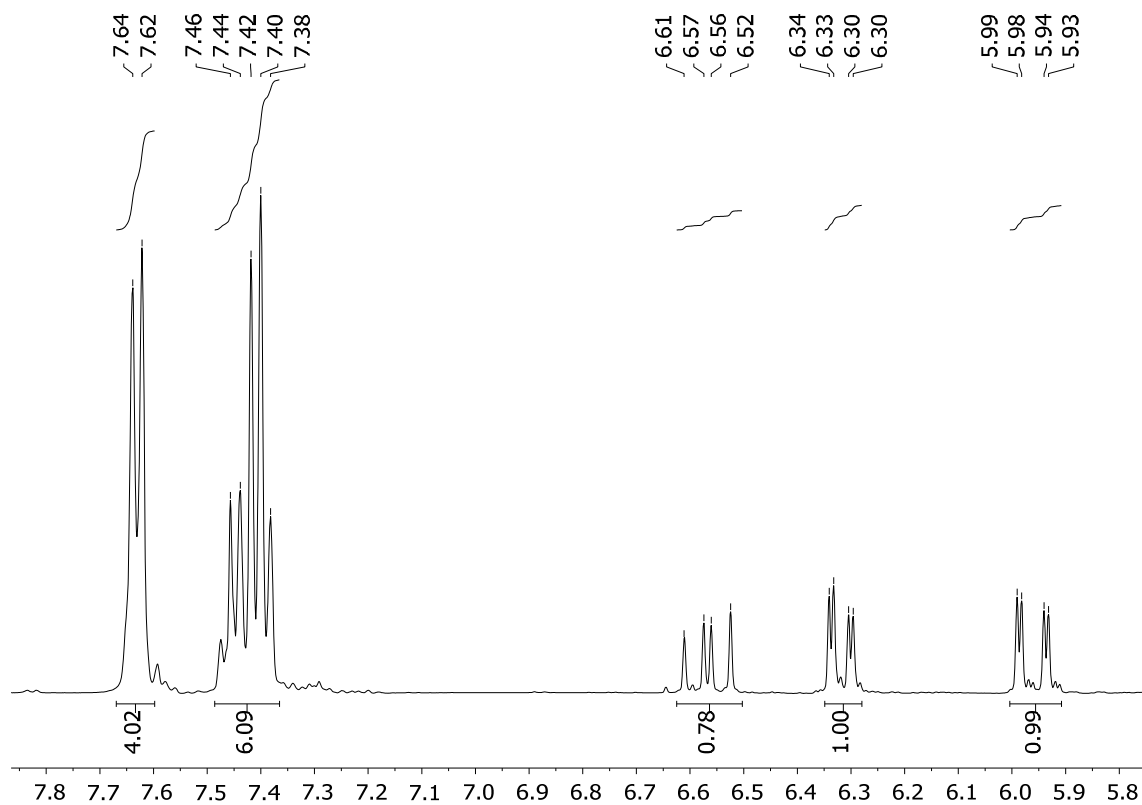


Figure S7: ^1H NMR spectrum of $\text{K}[\text{Ge}_9(\text{SiPh}_2\text{CH}=\text{CH}_2)_3]$ (**3**) in thf-d_8 .

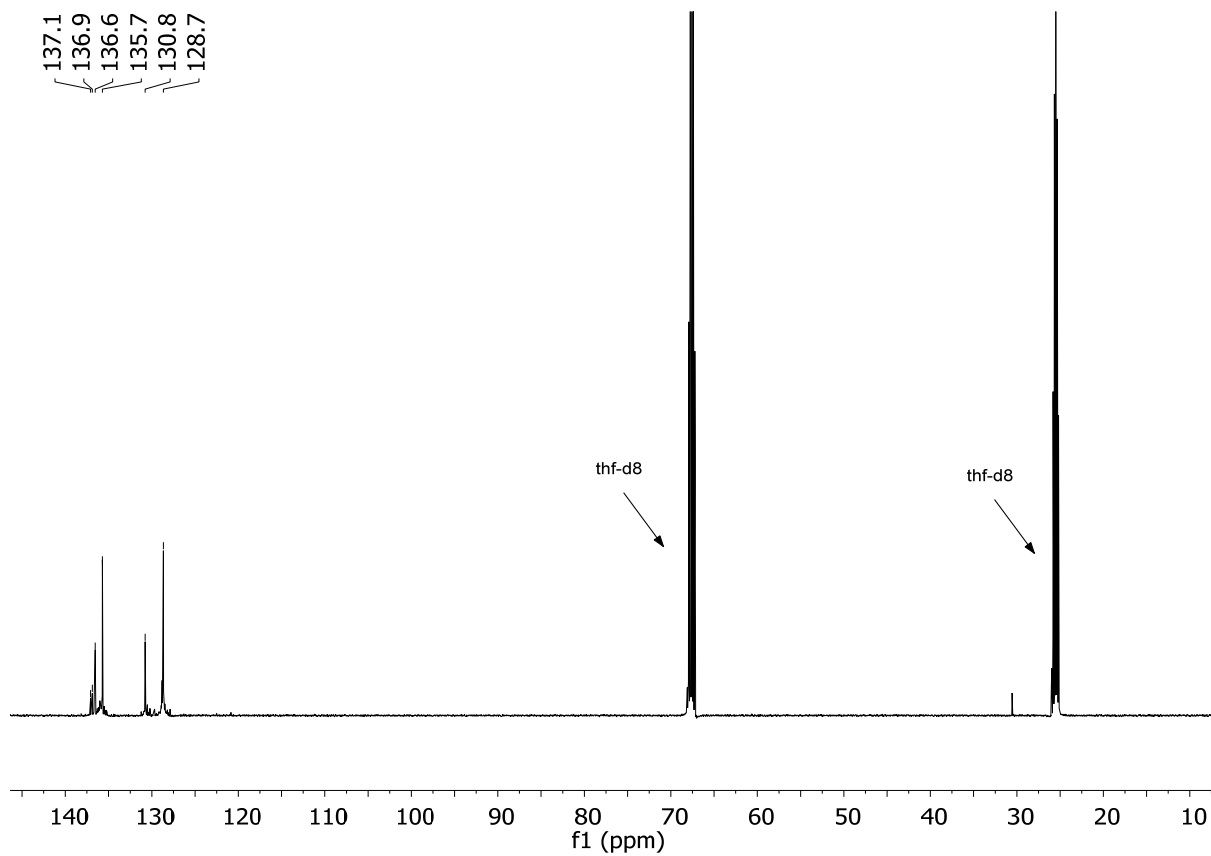


Figure S8: ^{13}C NMR spectrum of $\text{K}[\text{Ge}_9(\text{SiPh}_2\text{CH}=\text{CH}_2)_3]$ (**3**) in thf-d_8 .

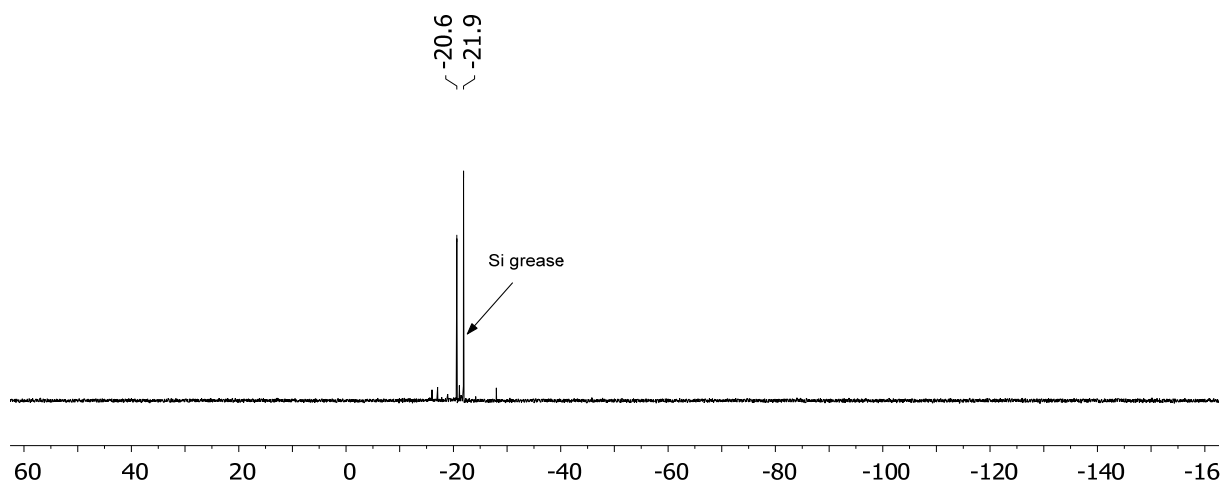


Figure S9: ^{29}Si NMR spectrum of $\text{K}[\text{Ge}_9(\text{SiPh}_2\text{CH}=\text{CH}_2)_3]$ (**3**) in thf-d_8 .

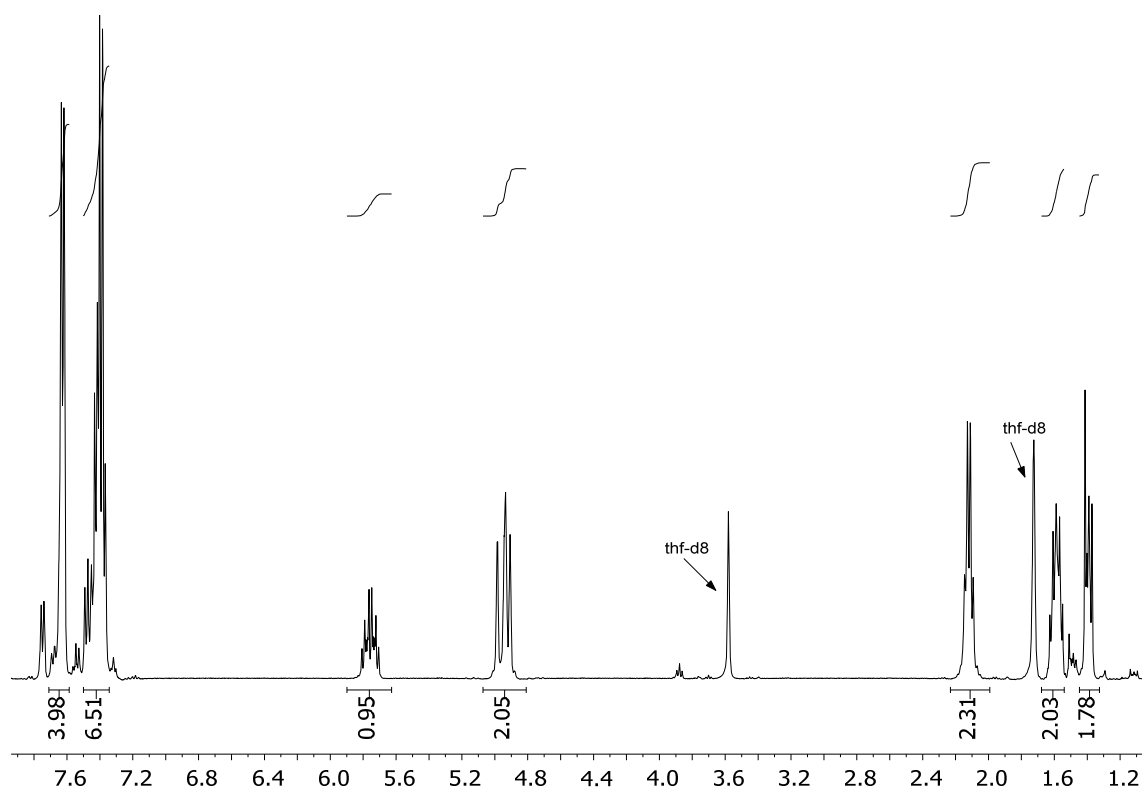


Figure S10: ^1H NMR spectrum of $\text{K}[\text{Ge}_9\{\text{SiPh}_2(\text{CH}_2)_3\text{CH}=\text{CH}_2\}_3]$ (**4**) in thf-d_8 .

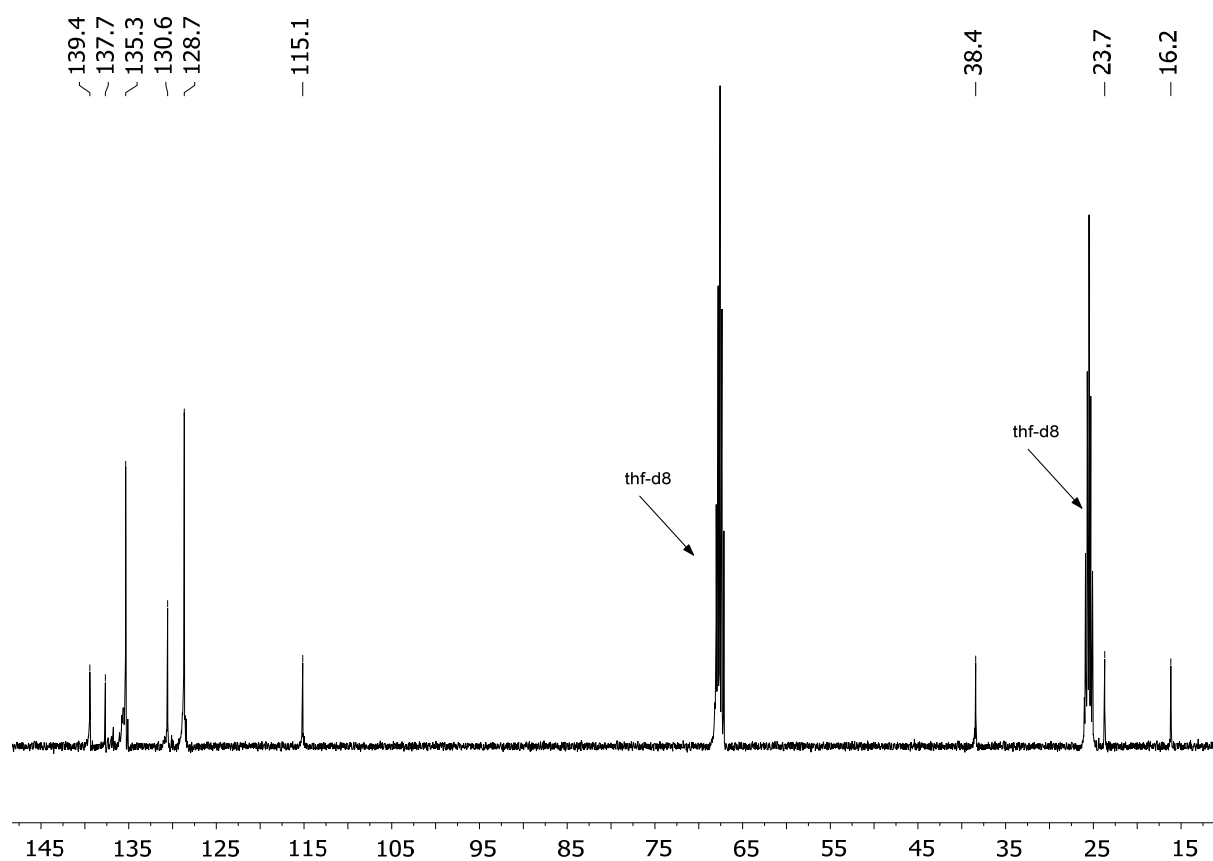


Figure S11: ^{13}C NMR spectrum of $\text{K}[\text{Ge}_9\{\text{SiPh}_2(\text{CH}_2)_3\text{CH}=\text{CH}_2\}_3]$ (**4**) in thf-d_8 .

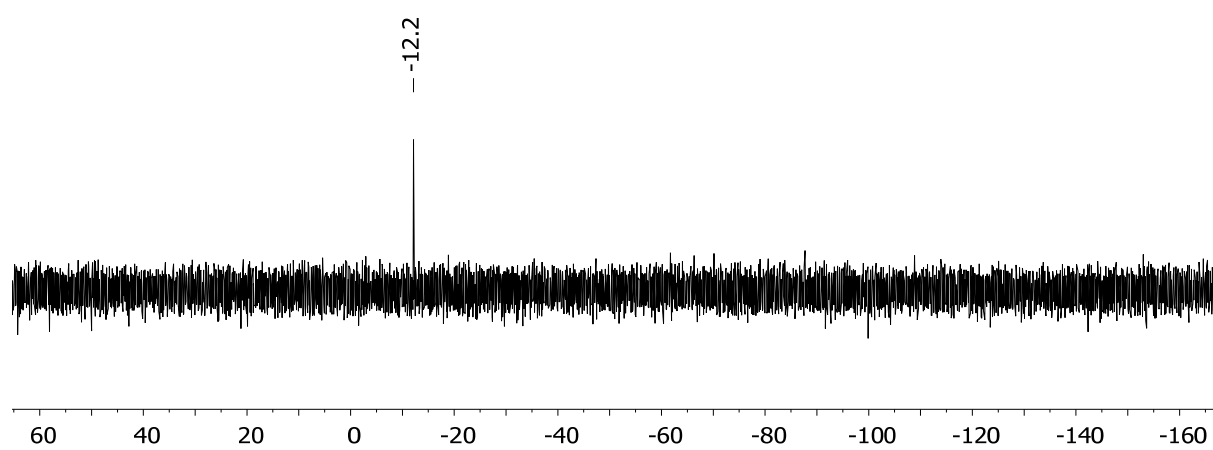


Figure S12: ^{29}Si NMR spectrum of $\text{K}[\text{Ge}_9\{\text{SiPh}_2(\text{CH}_2)_3\text{CH}=\text{CH}_2\}_3]$ (**4**) in thf-d_8 .

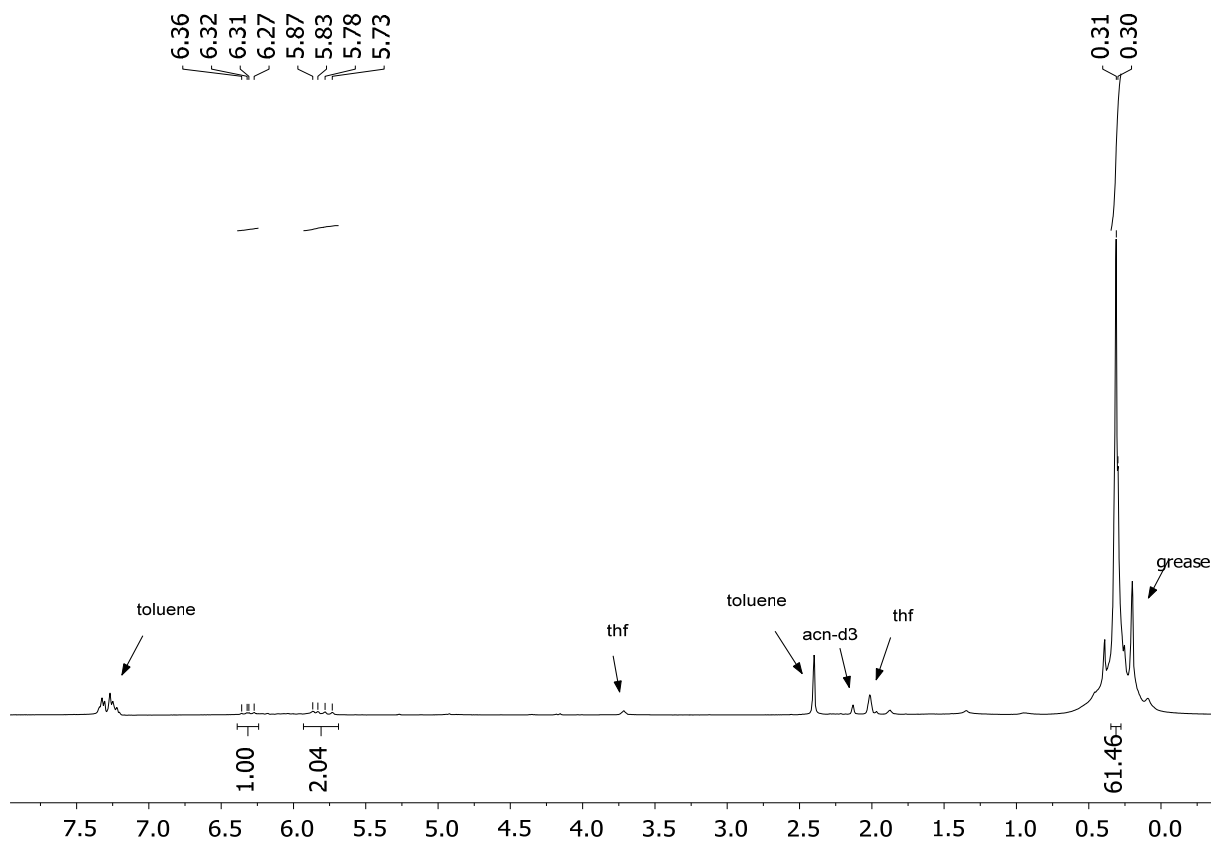


Figure S13: ^1H NMR spectrum of $\text{K}[\text{Ge}_9\{\text{Si}(\text{SiMe}_3)_3\}_2(\text{SiMe}_2\text{CH}=\text{CH}_2)]$ in acn-d_3 .

3. ESI-MS Spectra

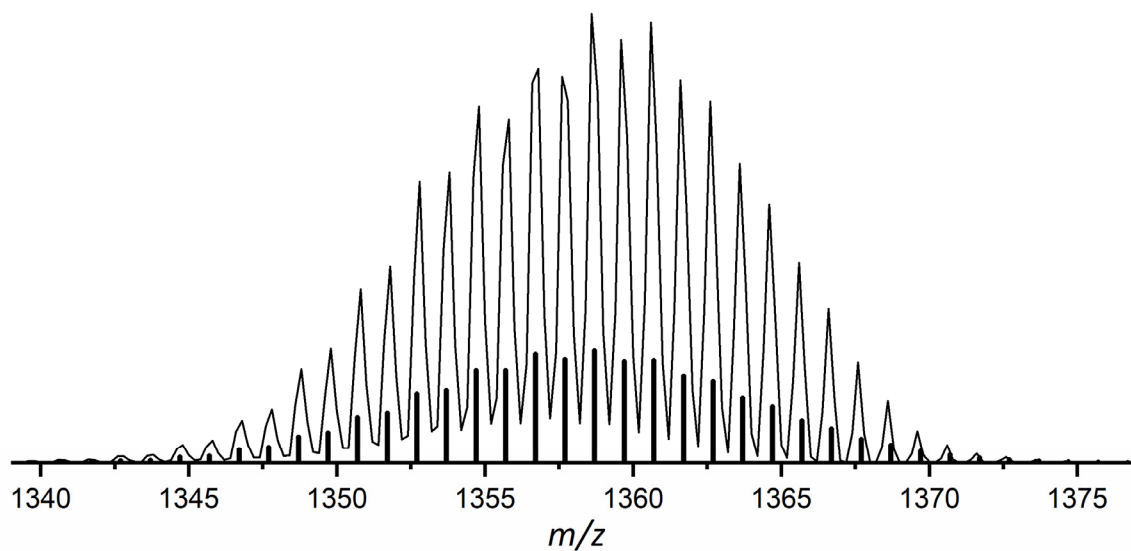


Figure S14: ESI-MS plot of $[\text{Ge}_9\{\text{Si}(\text{SiMe}_3)_3\}_2(\text{SiPh}_2\text{CH}=\text{CH}_2)]^-$ (1, $m/z = 1359$).

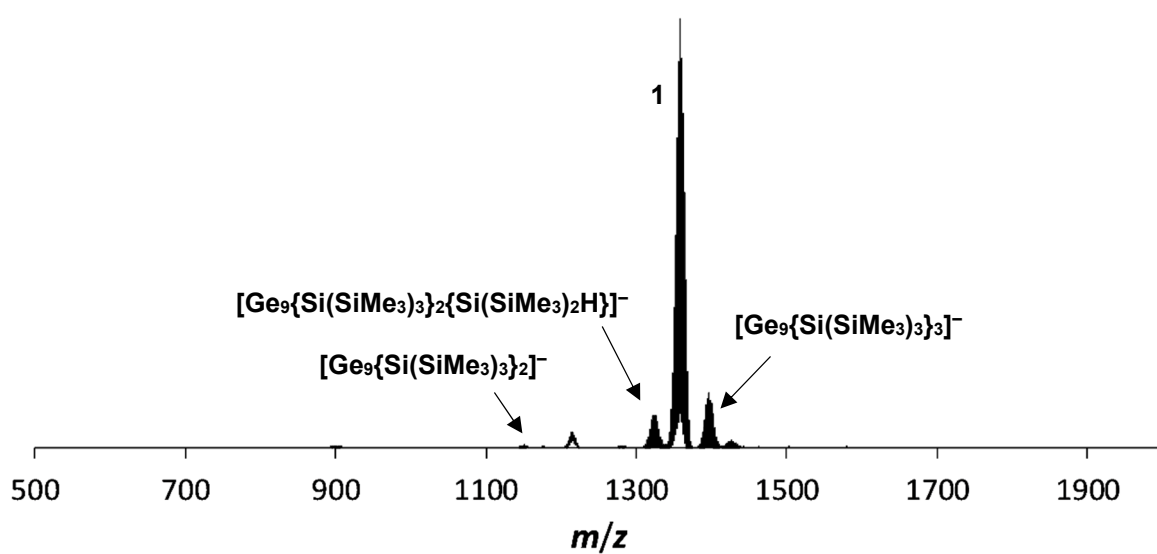


Figure S15: ESI-MS overview spectrum of $[\text{Ge}_9\{\text{Si}(\text{SiMe}_3)_3\}_2(\text{SiPh}_2\text{CH}=\text{CH}_2)]^-$ (1).

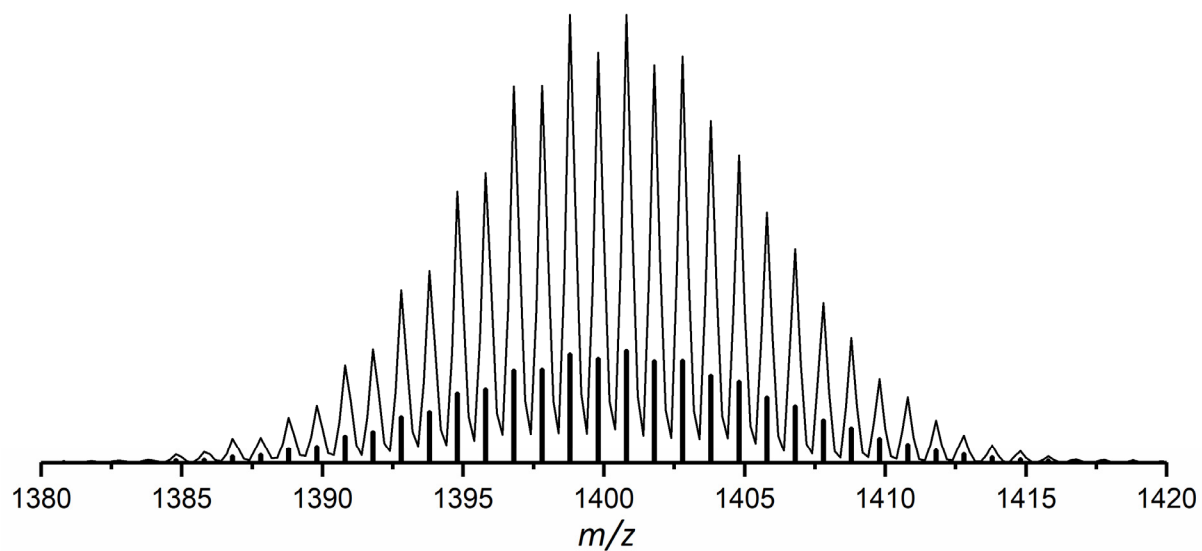


Figure S16: ESI-MS plot of $[\text{Ge}_9\{\text{Si}(\text{SiMe}_3)_3\}_2(\text{SiPh}_2(\text{CH}_2)_3\text{CH}=\text{CH}_2)]^-$ (**2**, $m/z = 1400$).

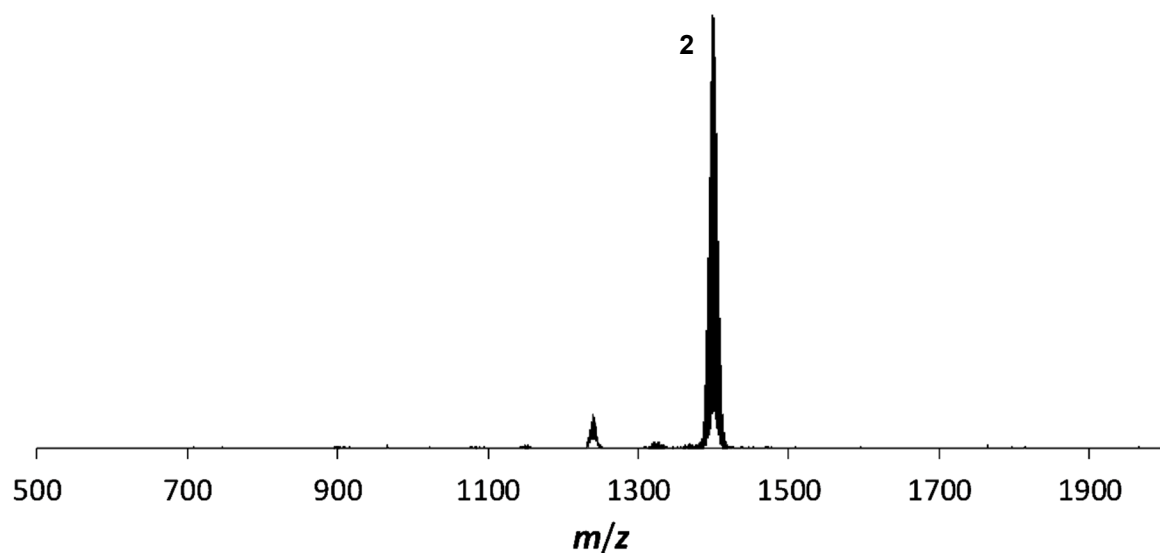


Figure S17: ESI-MS overview spectrum of $[\text{Ge}_9\{\text{Si}(\text{SiMe}_3)_3\}_2(\text{SiPh}_2(\text{CH}_2)_3\text{CH}=\text{CH}_2)]^-$ (**2**).

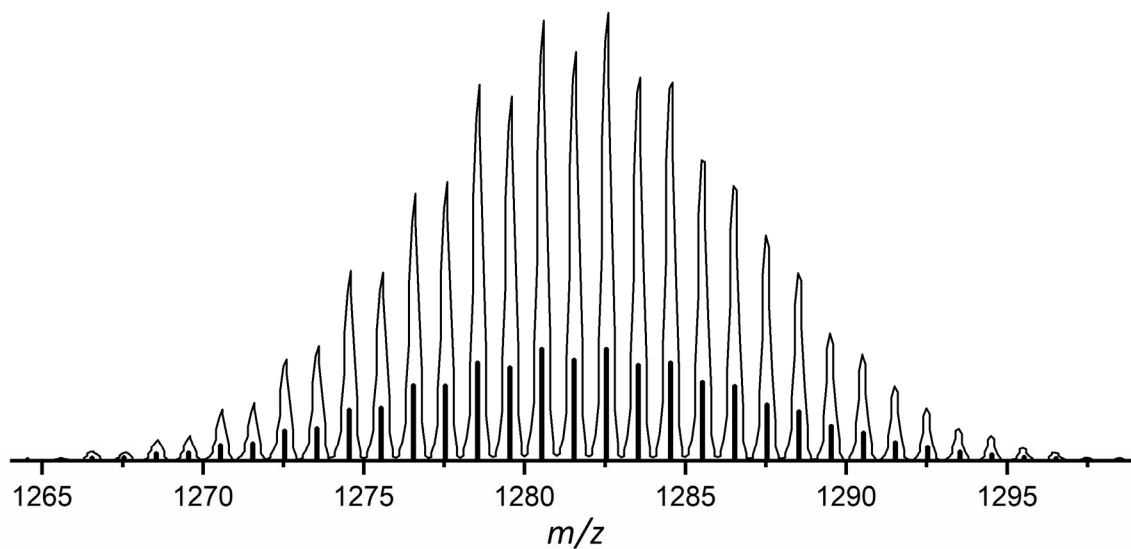


Figure S18: ESI-MS plot of $[\text{Ge}_9(\text{SiPh}_2\text{CH}=\text{CH}_2)_3]^-$ (**3**, $m/z = 1282$).

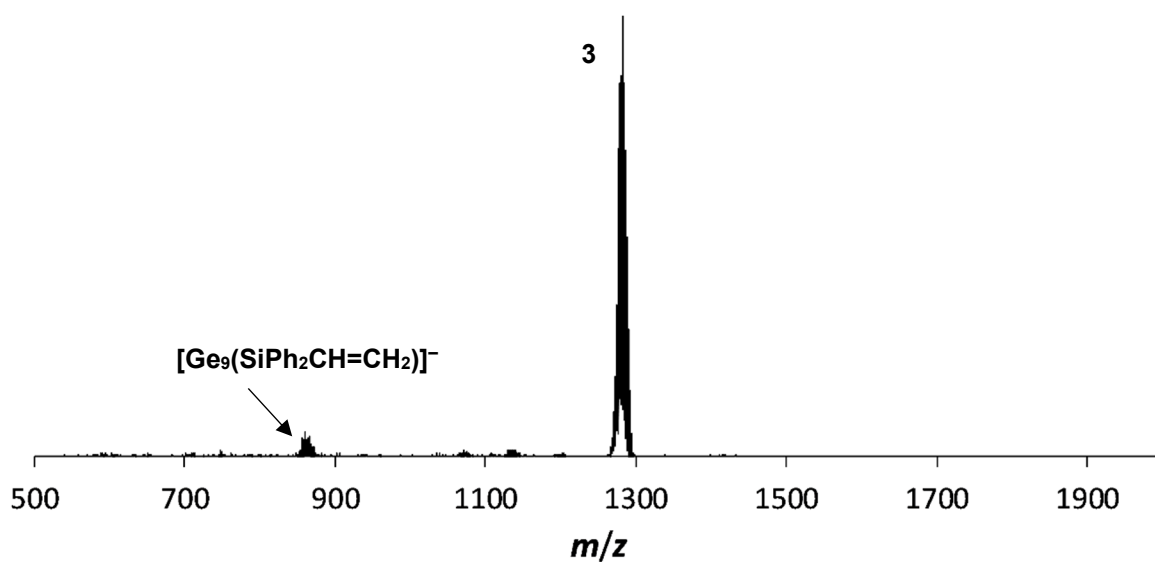


Figure S19: ESI-MS overview spectrum of $[\text{Ge}_9(\text{SiPh}_2\text{CH}=\text{CH}_2)_3]^-$ (**3**).

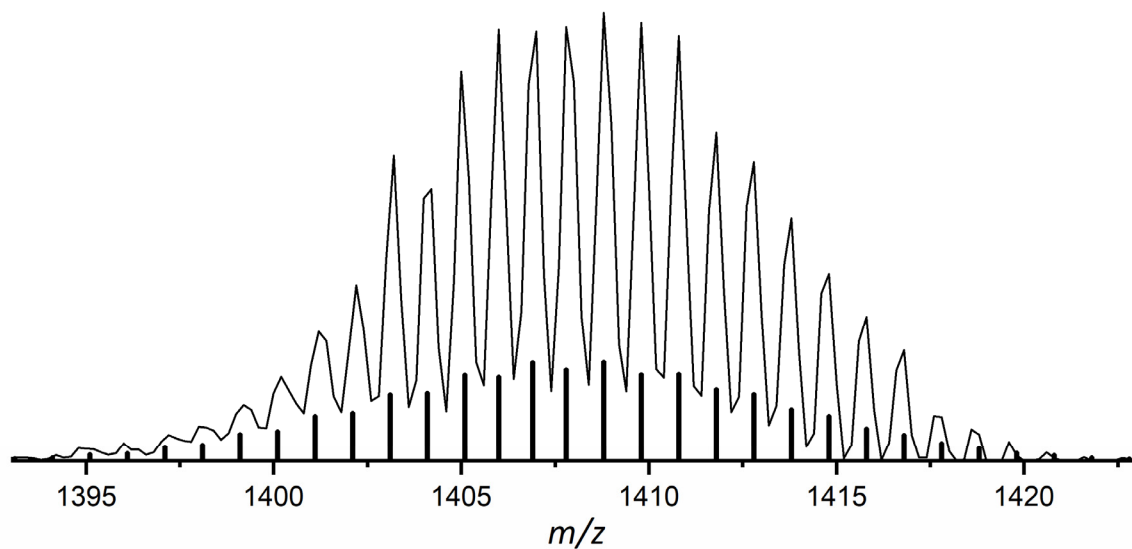


Figure S20: ESI-MS plot of $[\text{Ge}_9(\text{SiPh}_2\text{CH}=\text{CH}_2)_3]^-$ (**4**, $m/z = 1408$).

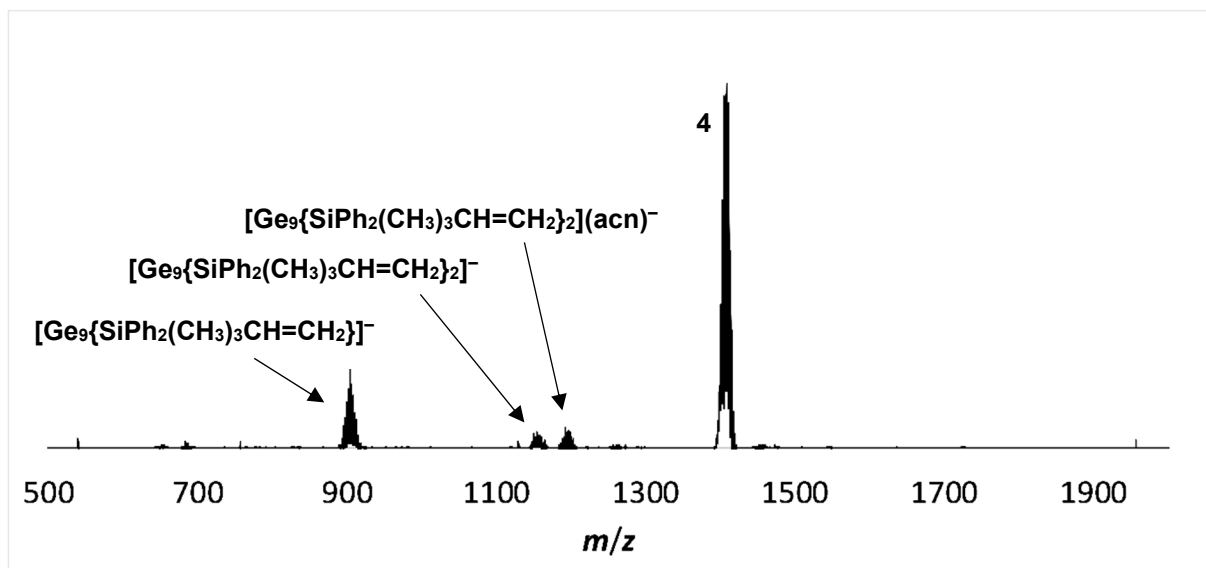


Figure S21: ESI-MS overview spectrum of $[\text{Ge}_9(\text{SiPh}_2\text{CH}=\text{CH}_2)_3]^-$ (**4**, $m/z = 1408$).

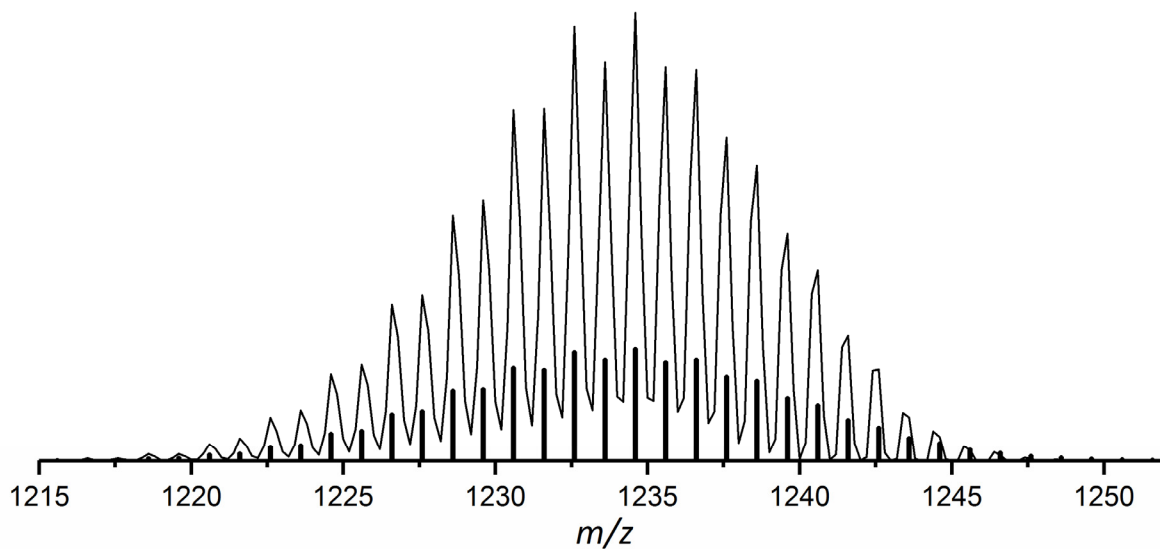


Figure S22: ESI-MS plot of $[\text{Ge}_9\{\text{Si}(\text{SiMe}_3)_3\}_2(\text{SiMe}_2\text{CH}=\text{CH}_2)]^-$ ($m/z = 1235$).

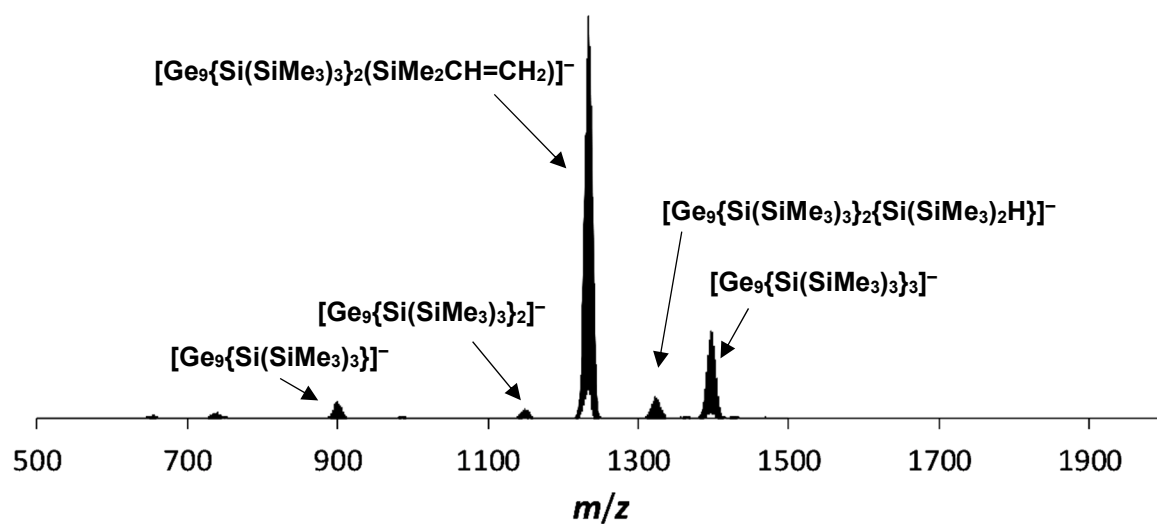


Figure S23: ESI-MS overview spectrum of $[\text{Ge}_9\{\text{Si}(\text{SiMe}_3)_3\}_2(\text{SiMe}_2\text{CH}=\text{CH}_2)]^-$.

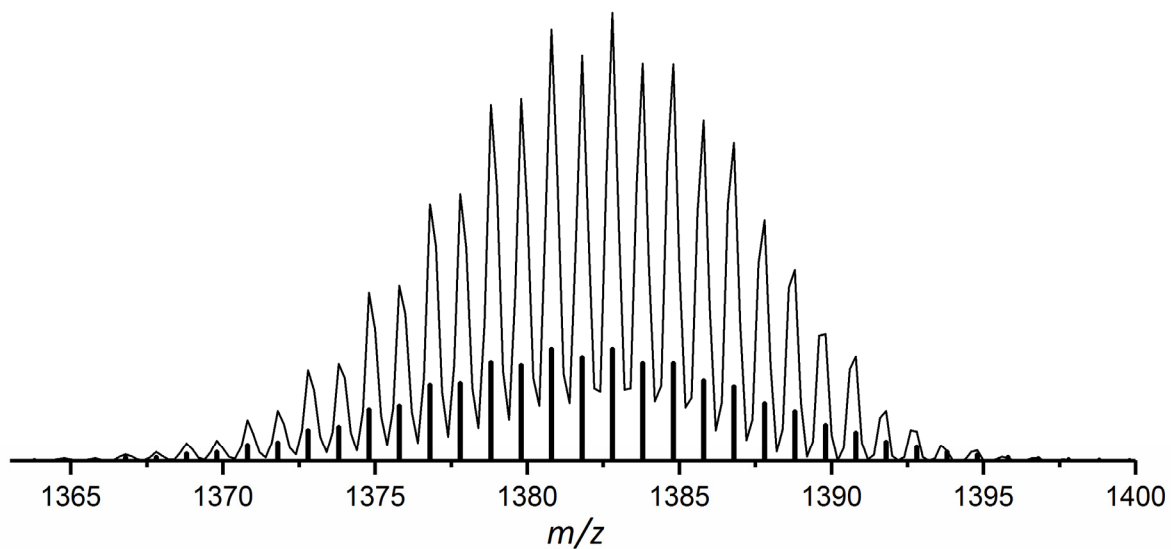


Figure S24: ESI-MS plot of $[\text{Ge}_9(\text{SiPh}_3)(\text{SiPh}_2\text{CH}=\text{CH}_2)]^-$ ($m/z = 1383$).

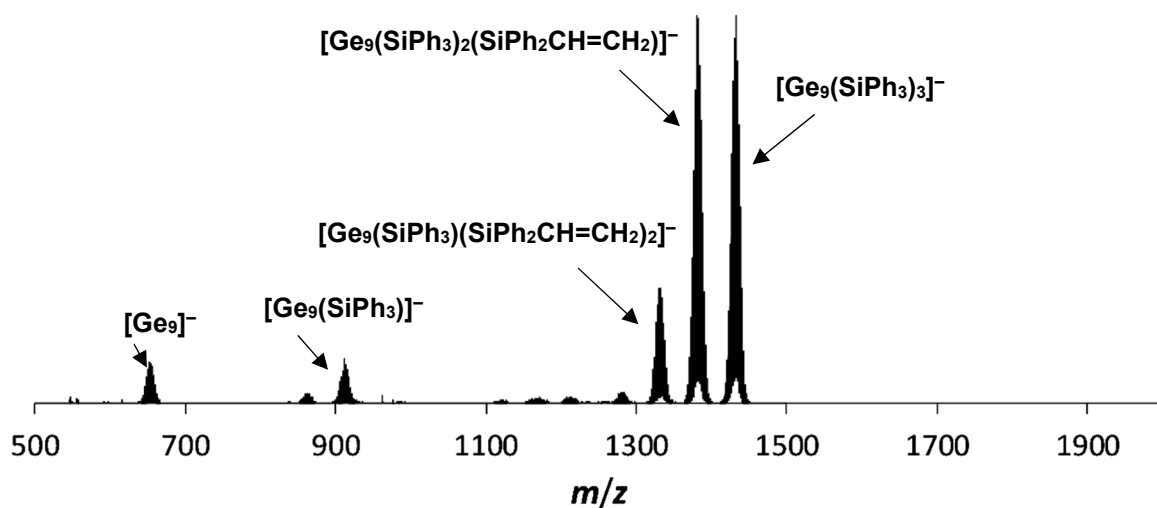


Figure S25: ESI-MS overview spectrum of $[\text{Ge}_9(\text{SiPh}_3)(\text{SiPh}_2\text{CH}=\text{CH}_2)]^-$.

4. IR and Raman spectra

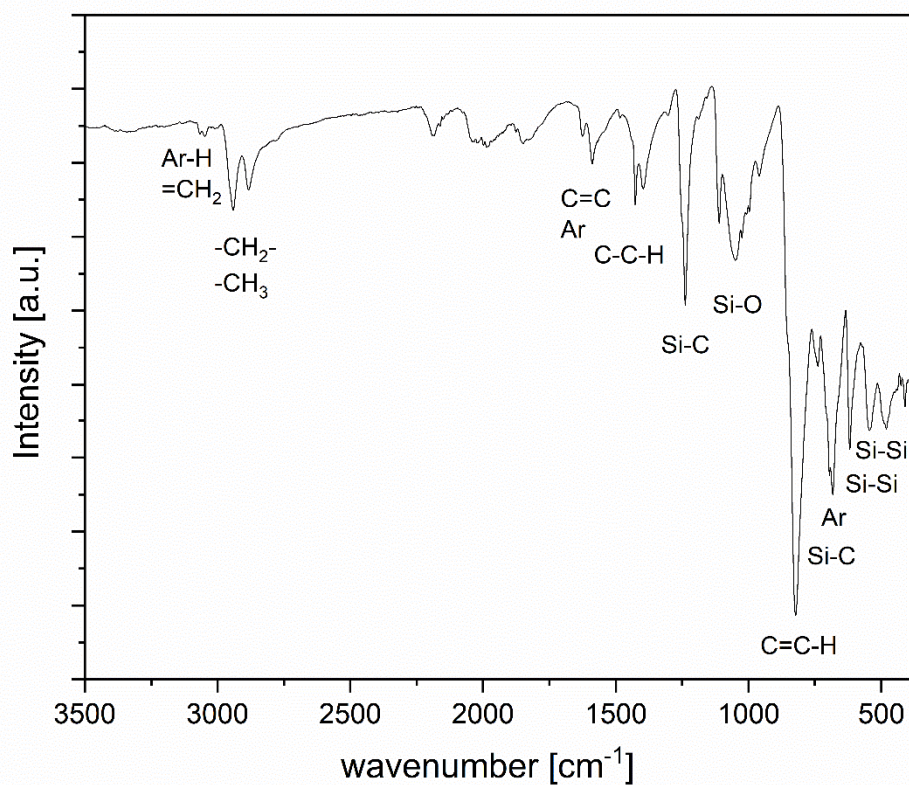


Figure S26: IR spectrum of $[\text{Ge}_9\{\text{Si}(\text{SiMe}_3)_3\}_2(\text{SiPh}_2\text{CH}=\text{CH}_2)]^-$ (1).

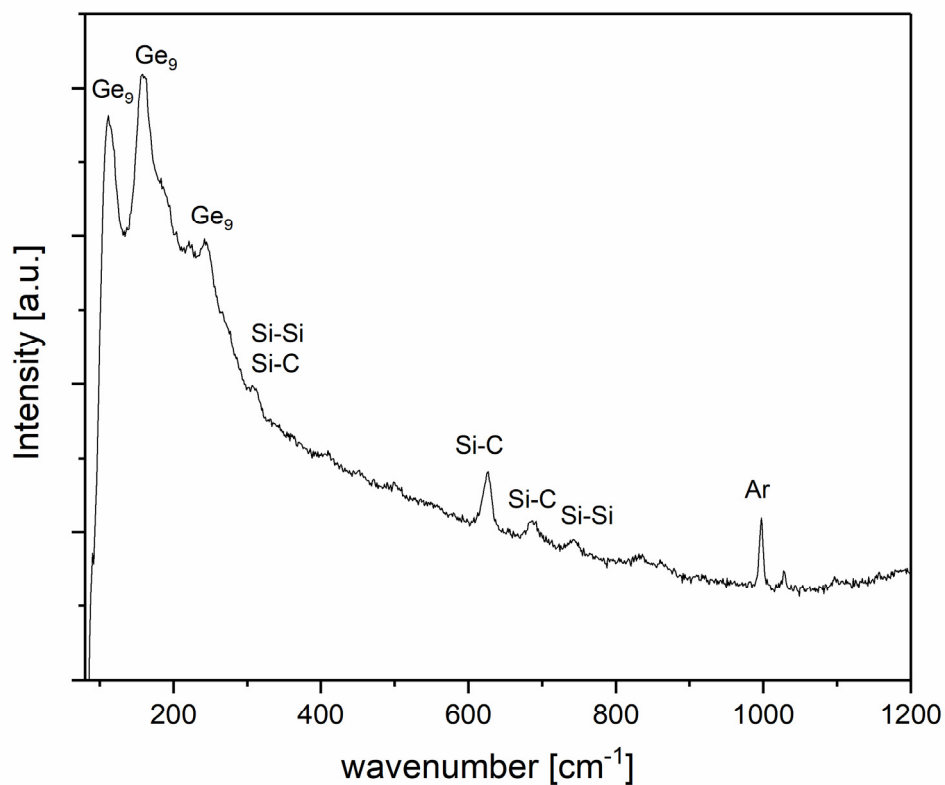


Figure S27: Raman spectrum of $[\text{Ge}_9\{\text{Si}(\text{SiMe}_3)_3\}_2(\text{SiPh}_2\text{CH}=\text{CH}_2)]^-$ (1).

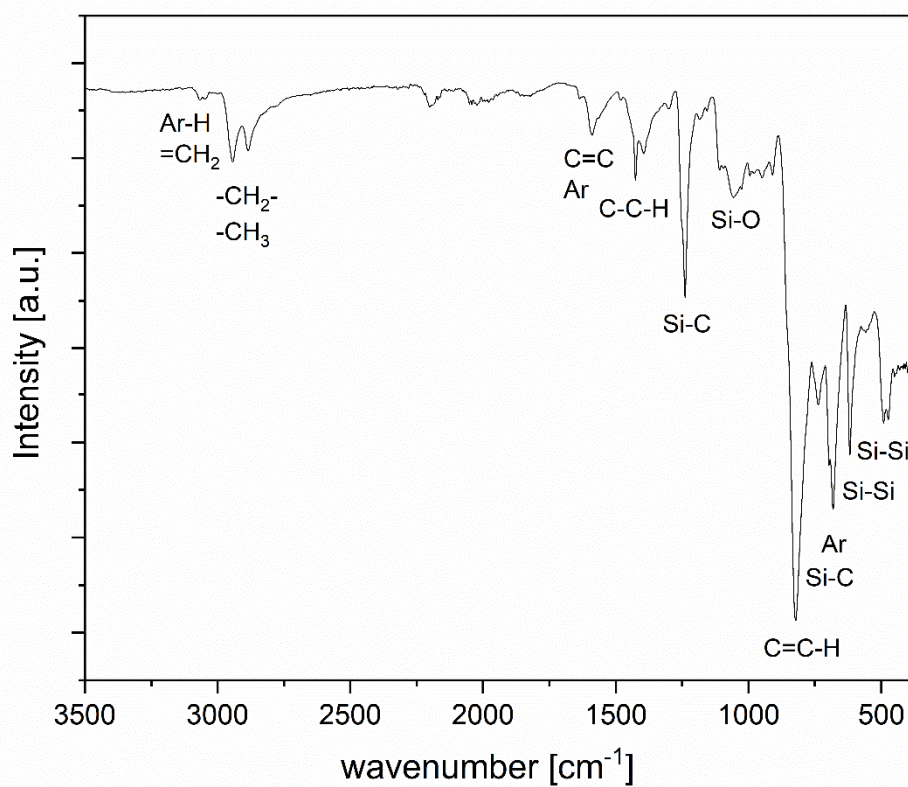


Figure S28: IR spectrum of $[\text{Ge}_9\{\text{Si}(\text{SiMe}_3)_3\}_2(\text{SiPh}_2(\text{CH}_2)_3\text{CH}=\text{CH}_2)]^-$ (**2**).

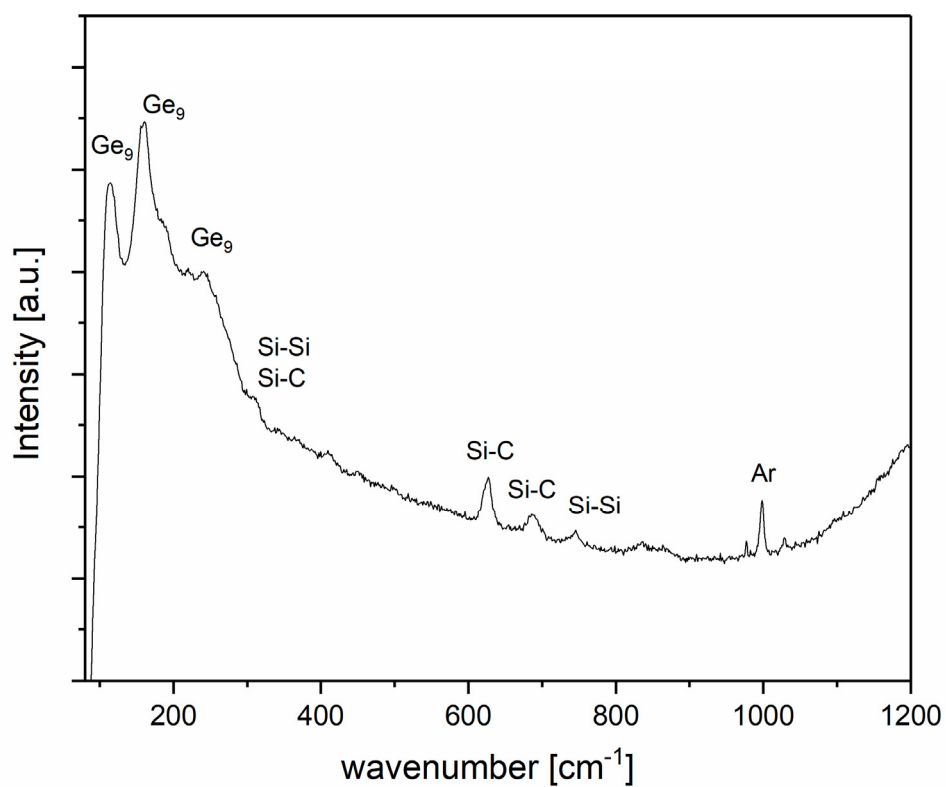


Figure S29: Raman spectrum of $[\text{Ge}_9\{\text{Si}(\text{SiMe}_3)_3\}_2(\text{SiPh}_2(\text{CH}_2)_3\text{CH}=\text{CH}_2)]^-$ (**2**).

5. XPS Investigations

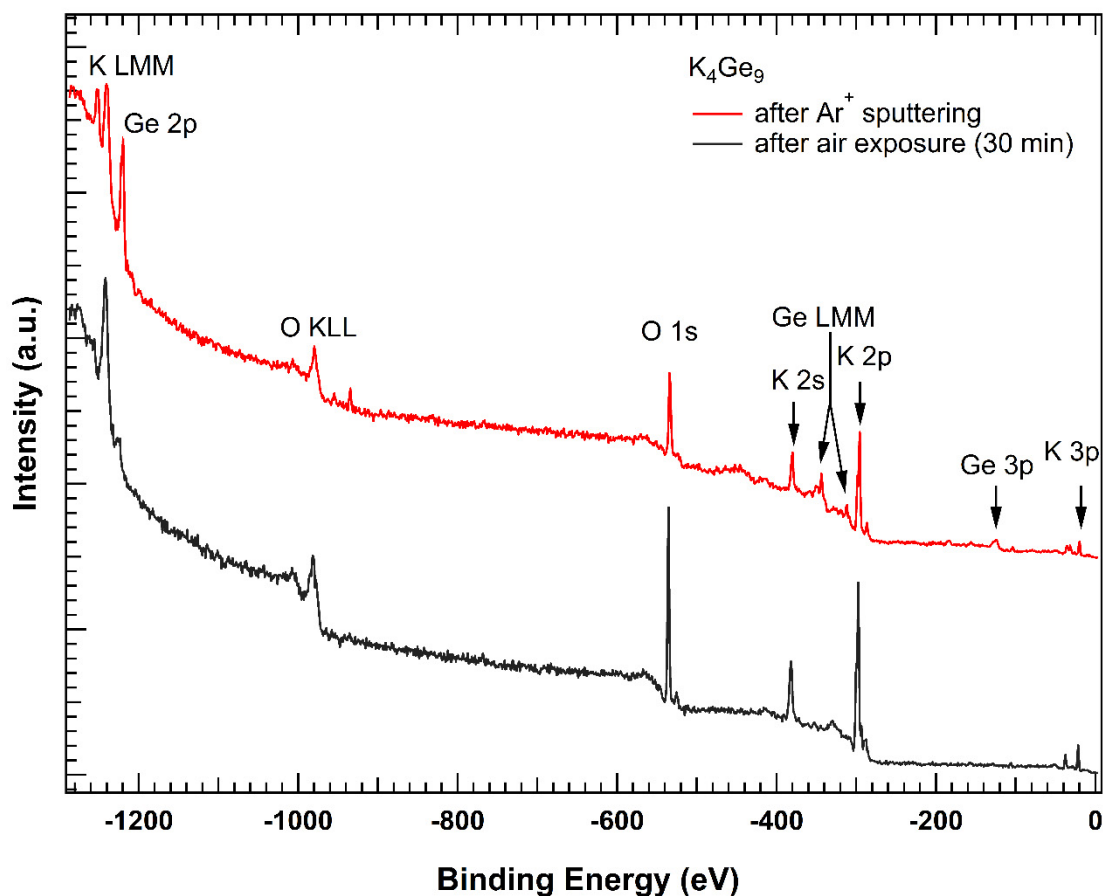


Figure S30: XP survey spectrum of K_4Ge_9 after Ar^+ sputtering (red) as well as after 30 min air exposure (black). The spectrum after sputtering shows signals of Ge (Ge 2p, Ge LMM, Ge 3p) and K (K 2s, K 2p, K 3p) as well as moderate O KVV and O 1s peaks indicating the presence of oxygen. After exposure to air, only potassium oxide is observed at the surface while photoemission from Ge-related core levels is blocked; this indicates complete decomposition of the compound.

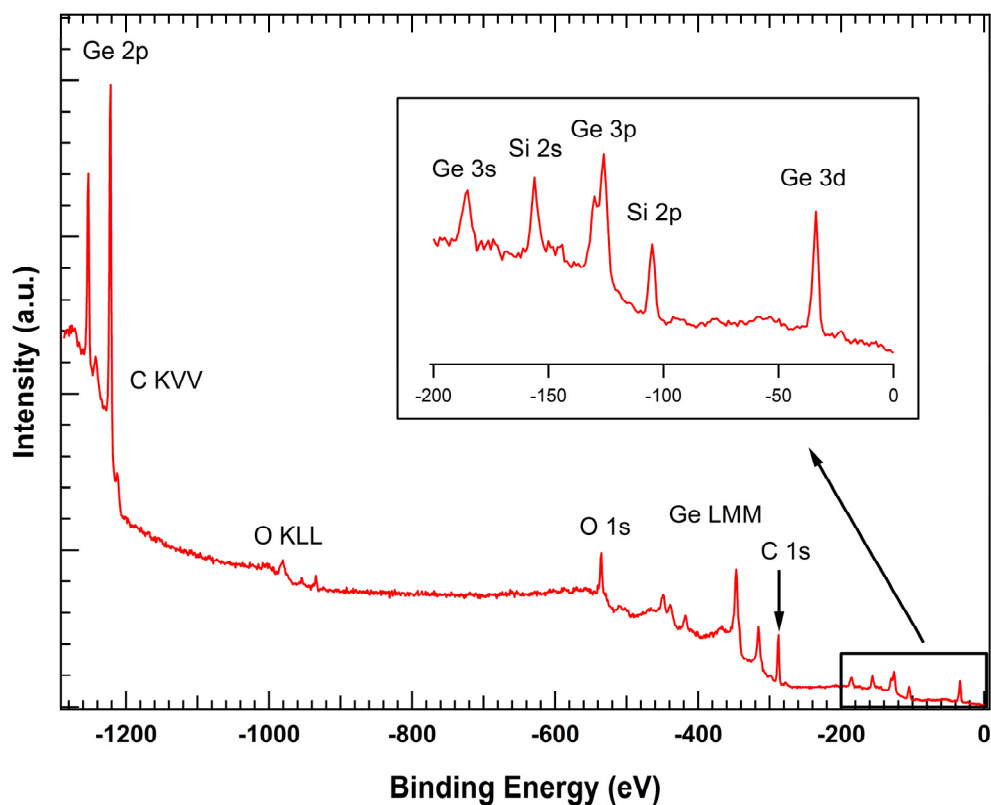


Figure S31: XP spectrum of **2**. The characteristic signals of Ge, Si, C and O are assigned. Due to low concentrations, K-related peaks could not be detected.

Table S1: Fractions of Ge(O), Ge(II) and Ge(IV) in the silylated cluster compounds and in K_4Ge_9 after Ar^+ sputtering as well as after air exposure. Oxidation states were identified by deconvolution of the Ge $2p_{3/2}$ peak for K_4Ge_9 and Ge 3d peak for the silylated clusters. Quantification was accomplished by comparison of the peak areas of the respective deconvoluted Ge species. The derived peak area fractions depend sensitively on the energy reference (Auger parameter relating to Ge(0)). The precision of the energy referencing of ± 0.1 eV influences the outcome of the peak deconvolution and, thus, introduces the given errors of about 5% for each Ge fraction.

Compound	Ge(0)	Ge(II)	Ge(IV)
1	72 \pm 7%	22 \pm 7%	6 \pm 2%
1 (after 30 min air)	65 \pm 7%	30 \pm 5%	5 \pm 2%
2	72 \pm 8%	23 \pm 6%	5 \pm 1%
K_4Ge_9	48 \pm 3%	24 \pm 4%	28 \pm 5%

6. Crystallographic details

Table S2: Selected crystallographic data of the crystal structures of **1** and **2**.

compound	1	2
formula	C ₇₈ H ₁₅₀ Ge ₁₈ K ₂ Si ₁₈	C ₃₉ H ₈₁ Ge ₉ KOSi ₉
fw (g·mol ⁻¹)	2978.41	1511.25
space group (no)	P21/c (14)	P21/n (14)
<i>a</i> (Å)	18.404(4)	9.5002(19)
<i>b</i> (Å)	27.045(5)	43.372(9)
<i>c</i> (Å)	27.036(5)	16.273(3)
α (deg)	90	90
β (deg)	100.80(3)	95.34(3)
γ (deg)	90	90
<i>V</i> (Å ³)	13218(5)	6676(2)
<i>Z</i>	4	4
<i>T</i> (K)	150(2)	150(2)
λ (Å)	0.71073	0.71073
ρ_{calcd} (g·cm ⁻³)	1.497	1.504
μ (mm ⁻¹)	4.282	4.242
collected reflections	172183	94371
independent reflections	25936	13120
<i>R</i> _{int}	0.1363	0.1276
parameters / restraints	1083 / 0	550 / 36
<i>R</i> ₁ [<i>I</i> > 2 σ (<i>I</i>) / all data]	0.065 / 0.129	0.066 / 0.114
<i>wR</i> ₂ [<i>I</i> > 2 σ (<i>I</i>) / all data]	0.140 / 0.167	0.164 / 0.196
goodness of fit	0.961	1.019
max./min. diff. el. density (e·Å ⁻³)	0.82 / -0.83	0.90 / -0.98

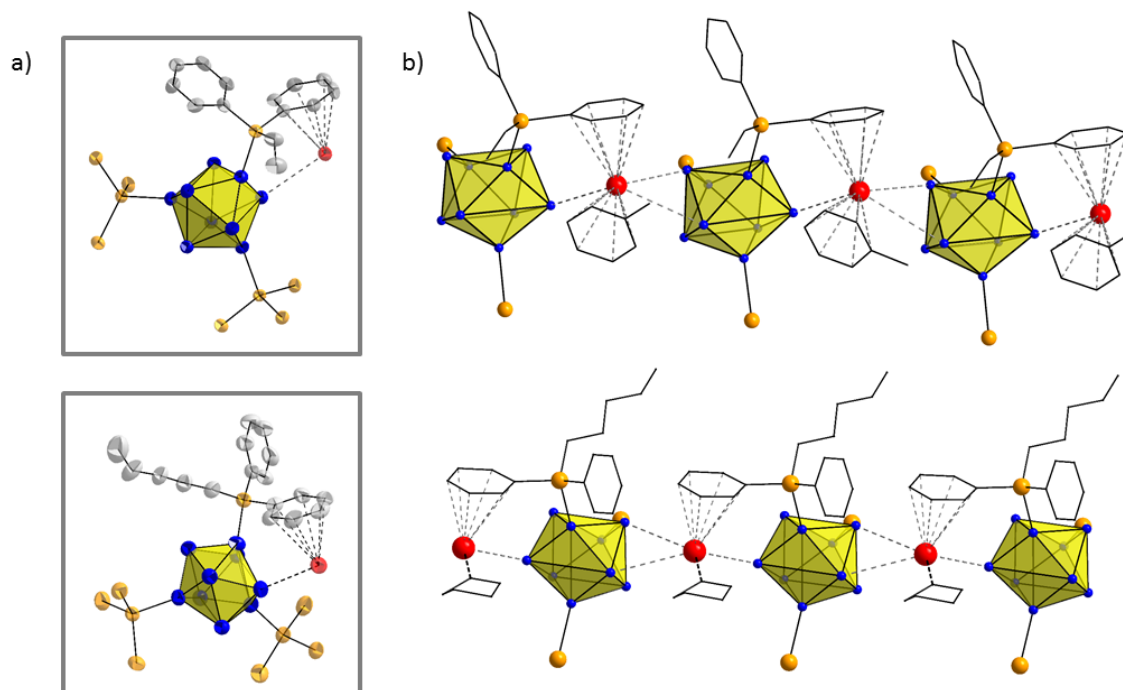


Figure S32: a) Molecular structures of the single unit in the single crystal structures of the compounds **1** (top) and **2** (bottom). The ellipsoids are shown at a probability level of 50%, Ge atoms are in blue, Si atoms in orange, C atoms in grey, and K atoms in red; [Ge₉] is shown as polyhedron; for reasons of clarity the methyl groups and H atoms are omitted). b) One-dimensional arrangement of compound **1**·(Tol)_{1.23} (top) and **2**·(thf) (bottom) formed by the coordination of one K atom to two clusters and one solvent molecule. Ge atoms are in blue, Si atoms in orange, K atoms in red, and C and O atoms are drawn as wire-sticks; [Ge₉] is shown as polyhedron.

7. Literature

1. O. Kysliak and A. Schnepf, *Dalton Trans.*, 2016, **45**, 2404-2408.
2. T. H. Johansen, K. Hagen, K. Hassler, A. D. Richardson, U. Pätzold and R. Stølevik, *J. Mol. Struct.*, 2000, **550**, 257-279.
3. G. M. Sheldrick, *Acta Crystallogr., Sect. C: Struct. Chem.* **2015**, *71*, 3-8.
4. A. L. Spek, *Acta Cryst.*, 2015, **C71**, 9-18.
5. MestreNova, Mestrelab Research, Version 11.0.4, 2017.
6. C. D. Wagner, *Faraday Discuss. Chem. Soc.*, 1975, **60**, 291-300.